Table 4 Reports for surgical removal of lung metastases of breast cancer

Author	Number of patients	Median age (range)	% of solitary metastasis	Curative surgery rate (%)	5-year survival (%)	10-year survival (%)	Median survival (months)
Lanza et al. [10]	41	55 (32–79)	73	90	50[a]	–	47[a]
Staren et al. [9]	33	–	82	–	36	–	55
Friedel et al. [16][b]	89	53 (23–78)	59	76	27	–	31
McDonald et al. [12]	60	58 (21–81)	52	67	38	8	42
Friedel et al. [8][c]	467	53 (21–87)	69	84	38	22	35

[a] For cases with complete resection

[b] Single institute

[c] Multi-institutes

advancements in diagnostic instrumentation such as CT and FDG-PET scanning have surely conduct a favourable results of surgical strategy.

Opposition to surgical treatment for metastatic breast cancer is based on the oncological viewpoint that it is a systemic disease. Most medical oncologists assert that the surgical treatment of metastatic disease is pointless in the presence of systemic foci. The value of the systemic approach cannot be underestimated, but the hopelessly low cure rate achieved by systemic treatment is unjustifiable. We must consider that the success of systemic drug therapy in the adjuvant setting [1, 2] and its inability to cure patients in the metastatic setting [3, 4]. This evidence indicates that cytostatics can overcome microscopic, but not clinically large metastatic foci, which might be due to the heterogeneous nature of cancer cells that become resistant to cytostatics [18].

Since cancer cells can acquire heterogeneity during cell division, the nature of resistance to cytostatics is essentially proportional to tumour size [14]. Smaller metastatic foci will retain more clonal identity and less heterogeneity, and will thus be more sensitive to anticancer drugs than larger metastasis foci [14]. Moreover, a smaller disease burden presumably requires fewer "logs" to kill [18], or might confer more kinetic sensitivity to anticancer drugs [19]. If these notions are correct, then clinically evident metastatic tumours should be removed where possible, since the remaining microscopic metastatic foci will be more sensitive to anticancer drugs approximating their use as an adjuvant. This concept represents the foundation for our treating metastatic breast cancer by surgery. The results of the present study support the notion that this strategy is beneficial.

In conclusion, the data from our limited series of patients suggest that surgical treatment for operable lung metastasis of breast cancer will prolong survival in specific subgroups of patients to a greater extent than standard systemic drug therapy alone. To ascertain the significance of surgical treatment, a prospective randomized trial should compare conventional systemic drug therapies with and without surgery.

References

1. Early Breast Cancer Trialist' Collaborative Group (1998) Polychemotherapy for early breast cancer: an overview of the randomised trials. Lancet 352:930–942
2. Early Breast Cancer Trialist' Collaborative Group (1998) Tamoxifen for early breast cancer: an overview of the randomised trials. Lancet 351:1451–1467
3. Greenberg PA, Hortobagyi GN, Smith TL, Ziegler LD, Frye DK, Buzdar AU (1996) Long-term follow-up of patients with complete remission following combination chemotherapy for metastatic breast cancer. J Clin Oncol 14:2197–2205
4. Nabholtz JM, Lindsay MA, Hugh J, Mackey J, Smylie M, Au HJ, Tonkin K, Allen M (1999) The academic global virtual concept in clinical cancer research and its application to breast cancer: the breast cancer International Research Group. Semin Oncol 26:4–8
5. Sledge GW (1996) Should we dream the impossible dream? The meaning of long-term survival in metastatic breast cancer. J Clin Oncol 14:2191–2193
6. Hortobagyi GN (2002) Can we cure limited metastatic breast canacer? J Clin Oncol 20:620–623
7. Friedel G, Pastprino U, Ginsberg RJ, Goldstraw P, Johnston M, Pass H, Putnam JB, Yoomes H (2002) Results of lung metastasectomy from breast cancer: prognostic criteria on the basis of 467 cases of the International Registry of Lung Metastases. Eur J Cardiothorac Surg 22:335–344
8. Staren ED, Salerno C, Rongione A, Witt TR, Faber LP (1992) Pulmonary resection for metastatic breast cancer. Arch Surg 127:1282–1284
9. Lanza LA, Natarajan G, Roth JA, Putnam JB (1992) Long-term survival after resection of pulmonary metastasis from carcinoma of the breast. Ann Thorac Surg 54:244–248
10. Martini N, McCormack PM (1998) Evolution of the surgical management of pulmonary metastases. Chest Surg Clin N Am 8:13–27
11. McDonald ML, Deschamps C, Ilstrup DM, Allen MS, Trastek VF, Pairolero PC (1994) Pulmonary resection for metastatic breast cancer. Ann Thorac Surg 58:1599–1602
12. Giordano SH, Buzdar AU, Smith TL, Kau SW, Yang Y, Hortobagyi GN (2004) Is breast cancer survival improving? Cancer 100:44–52
13. Gerrero RM, Stein S, Stadtmauer EA (2002) High-dose chemotherapy and stem cell support for breast cancer: where are we now? Drugs Aging 19:475–485

14. Goldie JH, Coldman AJ (1983) Quantitative model for multiple levels of drug resistance in clinical tumors. Cancer Treat Rep 67:923–931
15. Friedel G, Linder A, Toomes H (1994) The significance of prognostic factors for the resection of pulmonary metastases of breast cancer. Thorac Cardiovasc Surg 42:71–75
16. Bodzin GA, Staren ED, Faber PL (1998) Breast carcinoma metastases. Chest Surg Clin N Am 8:145–156
17. Schlappack OK, Baur M, Steger G, Dittrich C, Moser K (1988) The clinical course of lung metastases from breast cancer. Klin Wochenschr 66:790–795
18. Skipper HE, Schabel FM (1984) Tumor stem cell heterogeneity: implications with respect to classification of cancers by chemotherapeutic effect. Cancer Treat Rep 68:43–61
19. Norton L, Simon R (1986) The Norton-Simon hypothesis revisited. Cancer Treat Rep 70:163–169

Multiplex Reverse Transcription-PCR Screening for *EML4-ALK* Fusion Transcripts

Kengo Takeuchi,[1] Young Lim Choi,[3] Manabu Soda,[3] Kentaro Inamura,[1] Yuki Togashi,[1] Satoko Hatano,[1] Munehiro Enomoto,[3] Shuji Takada,[3] Yoshihiro Yamashita,[3] Yukitoshi Satoh,[2] Sakae Okumura,[2] Ken Nakagawa,[2] Yuichi Ishikawa,[1] and Hiroyuki Mano[3,4]

Abstract **Purpose:** EML4-ALK is a fusion-type protein tyrosine kinase that is generated by inv(2) (p21p23) in the genome of non – small cell lung cancer (NSCLC). To allow sensitive detection of *EML4-ALK* fusion transcripts, we have now developed a multiplex reverse transcription-PCR (RT-PCR) system that captures all in-frame fusions between the two genes.

Experimental Design: Primers were designed to detect all possible in-frame fusions of *EML4* to exon 20 of *ALK*, and a single-tube multiplex RT-PCR assay was done with total RNA from 656 solid tumors of the lung ($n = 364$) and 10 other organs.

Results: From consecutive lung adenocarcinoma cases ($n = 253$), we identified 11 specimens (4.35%) positive for fusion transcripts, 9 of which were positive for the previously identified variants 1, 2, and 3. The remaining two specimens harbored novel transcript isoforms in which exon 14 (variant 4) or exon 2 (variant 5) of *EML4* was connected to exon 20 of *ALK*. No fusion transcripts were detected for other types of lung cancer ($n = 111$) or for tumors from 10 other organs ($n = 292$). Genomic rearrangements responsible for the fusion events in NSCLC cells were confirmed by genomic PCR analysis and fluorescence *in situ* hybridization. The novel isoforms of EML4-ALK manifested marked oncogenic activity, and they yielded a pattern of cytoplasmic staining with fine granular foci in immunohistochemical analysis of NSCLC specimens.

Conclusions: These data reinforce the importance of accurate diagnosis of EML4-ALK – positive tumors for the optimization of treatment strategies.

Authors' Affiliations: [1]Division of Pathology, The Cancer Institute, [2]Department of Thoracic Surgical Oncology, Thoracic Center, Cancer Institute Hospital, Japanese Foundation for Cancer Research, Tokyo, Japan; [3]Division of Functional Genomics, Jichi Medical University, Tochigi, Japan; and [4]CREST, Japan Science and Technology Agency, Saitama, Japan

Received 4/19/08; revised 6/23/08; accepted 7/3/08.

Grant support: Grants-in-Aid for Scientific Research from the Ministry of Education, Culture, Sports, Science, and Technology of Japan and grants from the Japan Society for the Promotion of Science; from the Ministry of Health, Labor, and Welfare of Japan; from the National Institute of Biomedical Innovation; from the Smoking Research Foundation; and from the Vehicle Racing Commemorative Foundation.

The costs of publication of this article were defrayed in part by the payment of page charges. This article must therefore be hereby marked *advertisement* in accordance with 18 U.S.C. Section 1734 solely to indicate this fact.

Note: Supplementary data for this article are available at Clinical Cancer Research Online (http://clincancerres.aacrjournals.org/).

K. Takeuchi and Y.L. Choi contributed equally to this work.

Current address for Y. Satoh: Department of Thoracic Surgery, Kitasato University School of Medicine, Kanagawa 228-8520, Japan.

The nucleotide sequences of the *EML4-ALK* variant 4, 5a, and 5b cDNAs have been deposited in DDBJ/EMBL/Genbank under the accession numbers AB374363, AB374364, and AB374365, respectively.

Requests for reprints: Kengo Takeuchi, Division of Pathology, The Cancer Institute, Japanese Foundation for Cancer Research, Tokyo 135-8550, Japan. Phone: 81-3-3520-0111; Fax: 81-3-3570-0558; E-mail: kentakeuchi-tky@umin.net.

doi:10.1158/1078-0432.CCR-08-1018

Chromosome rearrangement is a major mechanism giving rise to transforming potential in human cancers, especially in hematologic malignancies (1). A balanced translocation between chromosomes 9 and 22, for instance, generates an activated protein tyrosine kinase, BCR-ABL, that plays an essential role in the pathogenesis of chronic myeloid leukemia (2). The gene for another protein tyrosine kinase, ALK, is fused to those for NPM1 or other partner proteins in anaplastic lymphoma and soft tissue tumors, resulting in an increase in the kinase activity of ALK (3).

Mitelman et al. have suggested that chromosome translocations, in addition to being common in hematologic malignancies, are not rare in epithelial tumors (4, 5). These researchers also proposed that the genetic mechanisms underlying oncogenesis might not differ fundamentally between hematologic and epithelial malignancies, and that the current apparent difference in the frequency of chromosomal translocations between these two types of cancer is likely to disappear with the advent of new and more powerful investigative tools.

Consistent with this notion, recurrent chromosome rearrangements involving genes for ETS transcriptional factors have been identified in many cases of prostate cancer and may contribute to the hypersensitivity of prostate cancer cells to androgens (6, 7). In addition, we recently discovered another

Translational Relevance

EML4-ALK is a fusion-type protein-tyrosine kinase generated through a recurrent chromosome rearrangement, inv(2)(p21p23), observed in non–small cell lung cancer (NSCLC). Because both *EML4* and *ALK* genes are mapped to the short arm of chromosome 2 in opposite orientations, PCR with primer sets flanking the fusion points of the two genes would not produce any specific products from cells without inv(2)(p21p23). Reverse transcription (RT)-PCR for the fusion point would, therefore, become a highly sensitive and accurate means to detect tumors positive for *EML4-ALK*. Such analyses may detect small amounts of cancer cells in sputa from individuals with NSCLC at early clinical stages. Because several isoforms have been already reported for *EML4-ALK*, it is mandatory to detect all isoforms of the fusion kinase in a sensitive and reliable way. Toward this goal, we here developed a single-tube multiplex RT-PCR screening system to capture all possible isoforms of EML4-ALK. Examination of various tumor samples (n = 656) with our multiplex RT-PCR has indeed identified 11 specimens positive for the variants of EML4-ALK only among lung adenocarcinoma (n = 253). Our system, thus, paves a way for a sensitive molecular detection of this intractable disorder at early curable stages.

recurrent chromosome translocation in non–small cell lung cancer (NSCLC; ref. 8), a major cause of cancer deaths in humans. A small inversion within the short arm of chromosome 2, inv(2)(p21p23), was found to be present in <10% of NSCLC cases and to give rise to a novel fusion-type tyrosine kinase, EML4-ALK, that exhibited marked transforming activity *in vitro* (8). Transgenic mice that specifically express EML4-ALK in lung epithelial cells were also found to develop hundreds of adenocarcinoma nodules in both lungs at only a few weeks after birth, and such nodules disappeared rapidly in response to oral administration of a specific inhibitor of the catalytic activity of ALK.[5] These data thus indicate that EML4-ALK plays a pivotal role in malignant transformation in lung cancer, and they suggest that chemical compounds that inhibit the tyrosine kinase activity of EML4-ALK may provide an effective treatment for EML4-ALK–positive lung cancer. The selection of suitable drugs for individuals with lung cancer will thus require accurate determination of the absence or presence of the *EML4-ALK* fusion gene in biopsy specimens.

Given that *EML4* and *ALK* map in opposite orientations within the short arm of chromosome 2, reverse transcription-PCR (RT-PCR) analysis with primers designed to amplify the fusion points of *EML4-ALK* transcripts would not be expected to yield specific products from normal cells or cancer cells without inv(2)(p21p23). Such analysis should thus provide a highly reliable and sensitive means to detect *EML4-ALK* in clinical specimens. Given that sputum has been shown to be a suitable specimen for such molecular diagnosis of *EML4-ALK* positivity (8), detection of *EML4-ALK*–positive cells by RT-PCR analysis of sputa may be effective for the identification of lung cancer at early clinical stages. The accurate diagnosis of *EML4-ALK*–positive tumors, however, will require that all isoforms of *EML4-ALK* are detected.

The fusion of intron 13 or 20 of *EML4* to intron 19 of *ALK* gives rise to variant 1 or 2 of *EML4-ALK*, respectively (8). We have recently discovered another isoform (variant 3) of *EML4-ALK* in which intron 6 of *EML4* is ligated to intron 19 of *ALK* (9). Theoretically, in addition to such fusion of exons 6, 13, and 20 of *EML4*, an in-frame fusion to exon 20 of *ALK* can occur with exons 2, 18, or 21 of *EML4*. Given that the amino-terminal coiled-coil domain of EML4 is responsible for the dimerization and constitutive activation of EML4-ALK (8) and that exon 2 of *EML4* encodes the entire coiled-coil domain, all of these possible fusion genes would encode EML4-ALK proteins containing the coiled-coil domain and therefore likely produce oncogenic EML4-ALK kinases.

To establish a highly sensitive and accurate PCR-based screening system for *EML4-ALK*–positive cancer, we have now developed a high-throughput multiplex RT-PCR assay for the detection of all potential *EML4-ALK* in-frame fusion transcripts. Among a consecutive series of lung adenocarcinoma specimens (n = 253) as well as other solid tumor samples (n = 403), we have now identified a total of 11 lung adenocarcinoma specimens positive for *EML4-ALK*, two of which harbor previously unidentified fusion mRNAs.

Materials and Methods

Clinical samples and RNA extraction. This study was done with clinical samples from 253 lung adenocarcinomas, 90 other NSCLCs (71 squamous cell carcinomas, 7 adenosquamous carcinomas, 7 large cell carcinomas, 2 pleomorphic carcinomas, and 3 large cell endocrine carcinomas), 21 small cell lung carcinomas, 50 breast carcinomas, 46 renal cell carcinomas, 48 colon carcinomas, 13 prostate carcinomas, 29 urothelial carcinomas, 33 gastric carcinomas, 10 uterine carcinomas, 9 hepatocellular carcinomas, 8 pancreatic carcinomas, and 46 malignant fibrous histiocytomas. All specimens were collected with the approval of the ethical committee at the Cancer Institute Hospital (Tokyo, Japan) and with the informed consent of individuals undergoing surgery from May 1995 to July 2003. The NSCLC cases were consecutive and spanned a period of 19 mo. Histologic diagnosis of NSCLC was made according to the WHO classification (10). All lesions were grossly dissected, rapidly frozen in liquid nitrogen, and stored at −80°C until RNA extraction with an RNeasy Mini Kit (Qiagen). RNA quality and the absence of contamination with genomic DNA were verified by formaldehyde-agarose gel electrophoresis.

Multiplex RT-PCR analysis and nucleotide sequencing. Total RNA was subjected to RT with random primers and SuperScript III reverse transcriptase (Invitrogen). For detection of *EML4-ALK* fusion cDNAs, multiplex PCR analysis was done with AmpliTaq Gold DNA polymerase (Applied Biosystems), the forward primers EML4 72F (5′-GTCAGCTCTTGAGTCACGAGTT-3′) and Fusion-RT-S (5′-GTGCAGTGTTTAGCATTCTTGGGG-3′), and the reverse primer ALK 3078RR (5′-ATCCAGTTCGTCCTGTTCAGAGC-3′). The *GAPDH* cDNA was amplified by PCR with the primers 5′-GTCAGTGGTGGACCTGACCT-3′ and 5′-TGAGCTTGACAAAGTGGTCG-3′. For amplification of *EML4-ALK* fusion cDNAs, the samples were incubated at 94°C for 10 min and then subjected to 35 cycles of denaturation at 94°C for 1 min, annealing at 64°C for 1 min, and polymerization at 72°C for 1 min. For amplification of *GAPDH* cDNA, the samples were subjected to 35 cycles of 94°C for 1 min, 58°C for 30 s, and 72°C for 30 s. Virtual gel electrophoresis of multiplex RT-PCR products was done with a 2100 Bioanalyzer (Agilent Technologies).

[5] M. Soda et al., submitted for publication.

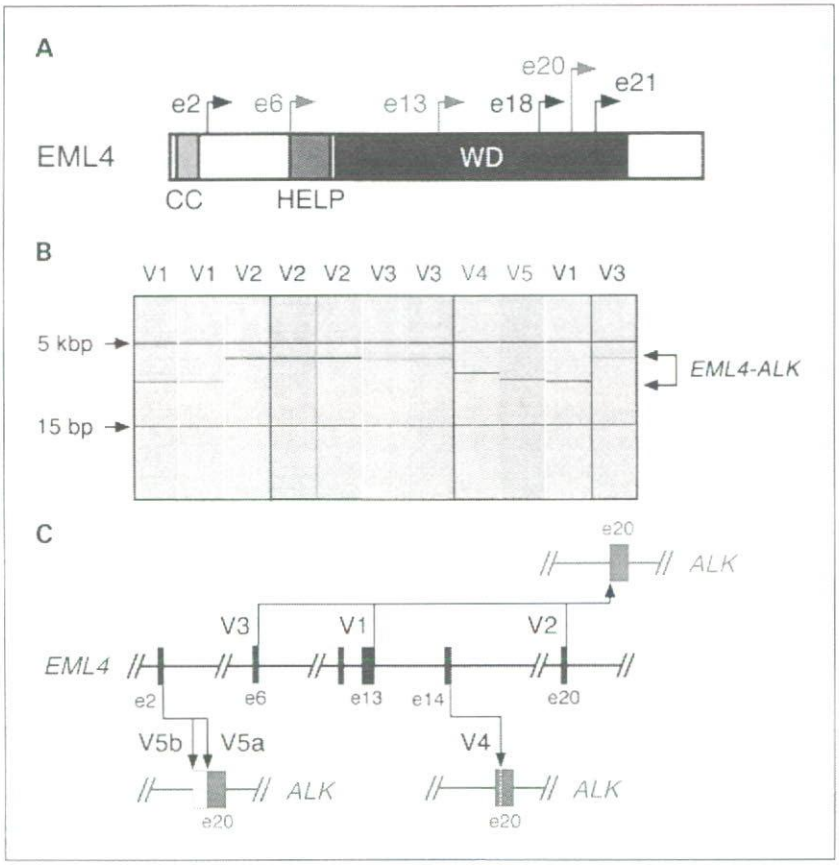

Fig. 1. Identification of *EML4-ALK* variants 4 and 5. *A*, schematic representation of the structure of EML4. The corresponding positions of exons (*e*) that can theoretically be fused in-frame to exon 20 of *ALK* are indicated by arrows, with known fusion points being denoted in red. CC, coiled-coil domain; HELP, hydrophobic EMAP (echinoderm microtubule-associated protein) – like protein domain; WD, WD repeats. *B*, virtual gel electrophoresis of multiplex RT-PCR products derived from lung adenocarcinoma specimens. Seven samples (*blue*) were known to harbor *EML-ALK* variants (*V*) 1, 2, or 3, whereas four samples were newly detected by multiplex RT-PCR. Two of the latter four specimens yielded PCR products corresponding to the newly identified variants 4 and 5. The positions of the fusion products of *EML4-ALK* are indicated on the right, and those of DNA size standards (5 kbp and 15 bp) are shown on the left. *C*, fusions between exons of *EML4* and *ALK*. Fusion of exons 6, 13, or 20 of *EML4* to exon 20 of *ALK* gives rise to variants 3, 1, and 2 of *EML4-ALK*, respectively. In addition, nucleotide sequencing of the PCR products shown in *B* revealed that exon 14 or 2 of *EML4* was fused to exon 20 of *ALK* in the cDNAs for *EML4-ALK* variants 4 and 5, respectively.

The primers used for direct amplification of the fusion points of individual cDNAs were 5′-AGGAGAGAACTCAGCGACACTACC-3′ and 5′-TCCACGCTCAAAAGTGCCAAGTCC-3′ for variant 4 and 5′-GCTTTCCCCGCAAGATGGACGG-3′ and 5′-AGCTTGCTCAGCTTG-TACTCAGGG-3′ for variant 5. Full-length cDNAs for *EML4-ALK* variants were amplified with PrimeSTAR DNA polymerase (Takara Bio) and the primers 5′-ACTCTGTCGGTCCGCTGAATGAAG-3′ and 5′-CCACGGTCTTAGGGATCCCAAGG-3′.

Fluorescence* in situ *hybridization analysis. Surgically resected lung cancer tissue was fixed in 20% formalin, embedded in paraffin, sectioned at a thickness of 4 μm, and placed on glass slides. The unstained sections were processed with a Histology FISH Accessory Kit (Dako), subjected to hybridization with fluorescently labeled bacterial artificial chromosome clone probes for *EML4* and *ALK* (GSP Laboratory) or for genomic regions upstream and downstream of the *ALK* break point (Dako), stained with 4,6-diamidino-2-phenylindole, and examined with a fluorescence microscope (BX51; Olympus).

Immunohistochemical analysis. Unstained paraffin-embedded sections were depleted of paraffin with xylene, rehydrated with a graded series of ethanol solutions, and then subjected to heat-induced antigen retrieval with Target Retrieval Solution pH 9.0 (Dako) before immunohistochemical staining with a mouse monoclonal antibody to ALK (ALK1, Dako) at a dilution of 1:20. Immune complexes were detected with the use of an EnVision+DAB system (Dako) with minor modifications.[6]

Transforming potential of EML4-ALK proteins. Protein analysis of EML4-ALK variants was done as described previously (8). In brief, the *EML4-ALK* variant 4, 5a, or 5b cDNAs were fused with an oligonucleotide encoding the FLAG epitope tag and inserted into the retroviral expression plasmid pMXS (11). The resulting plasmids and similar pMXS-based expression plasmids for EML4-ALK variant 1, variant 1(K589M), variant 2, variant 3a, and variant 3b were individually introduced into HEK293 cells. Lysates of the transfected cells were subjected to immunoprecipitation with antibodies to FLAG, and the resulting precipitates were subjected either to immunoblot analysis with the same antibodies or to an *in vitro* kinase assay with the YFF peptide (12). Mouse 3T3 fibroblasts were also infected with recombinant retroviruses for each of the EML4-ALK variants or wild-type ALK and were then cultured for 12 d for a focus formation assay. The same set of 3T3 cells was injected s.c. into nu/nu mice, and tumor formation was examined after 20 d.

Results

Multiplex RT-PCR screening for EML4-ALK fusion transcripts in lung adenocarcinoma. As described above, exons 2, 6, 13, 18, 20, and 21 of *EML4* may participate in an in-frame fusion to exon 20 of *ALK* (Fig. 1A). To identify all possible *EML4-ALK* fusion cDNAs in a single-tube experiment, we designed a mixture of two sense primers (one targeted to exon 2 and the other to exon 13 of *EML4*) and a single antisense primer (targeted to exon 20 of *ALK*) and did multiplex RT-PCR with these primers and total cDNA preparations from tumor specimens. The exon 2 primer for *EML4* would be expected to generate a PCR product of 458 bp with the exon 2 (*EML4*)-exon 20 (*ALK*) fusion cDNA or of 917 bp with the exon 6-exon 20 fusion cDNA (variant 3). In addition, the exon 13 primer for *EML4* would be expected to generate PCR products of 432, 999, 1,185, or 1,284 bp with the exon 13-exon 20 (variant 1), exon 18-exon 20, exon 20-exon 20 (variant 2), and exon 21-exon 20 fusion cDNAs, respectively.

[6] K. Takeuchi et al., manuscript in preparation.

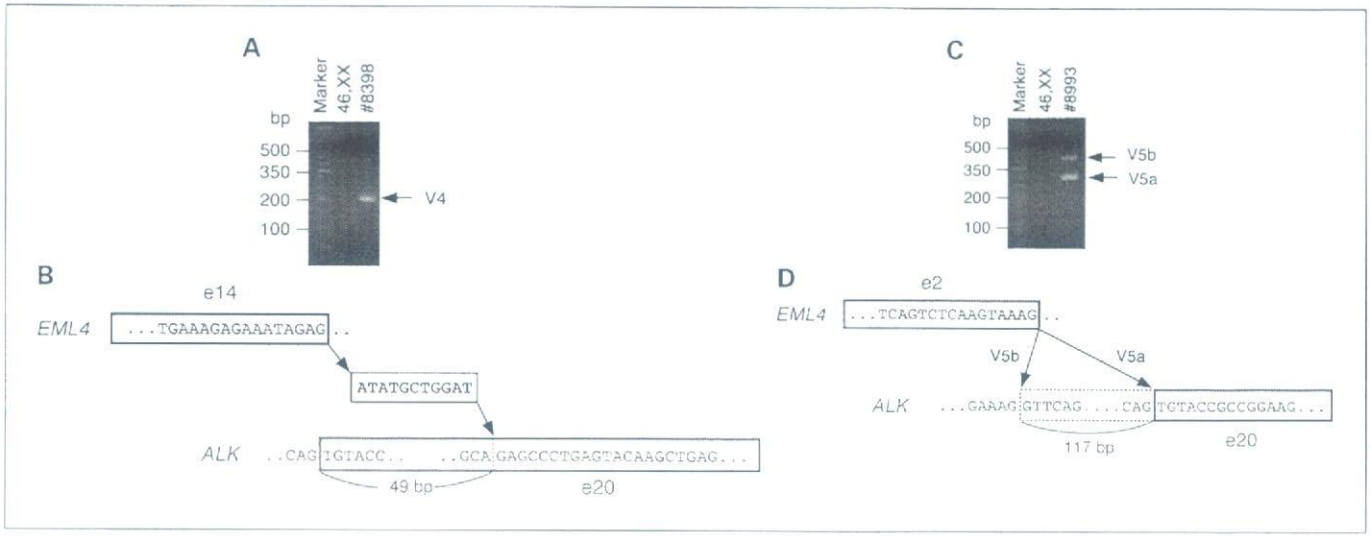

Fig. 2. Structure of *EML4-ALK* variant 4 and 5 cDNAs. *A*, RT-PCR amplification of the fusion point of *EML4-ALK* variant 4 mRNA in NSCLC specimen ID no. 8398 as well as in peripheral blood mononuclear cells of a female volunteer (46,XX). A PCR product of 203 bp corresponding to *EML4-ALK* variant 4 was specifically amplified from the tumor cells. The left lane contains DNA size standards (50-bp ladder). *B*, nucleotide sequencing of the PCR product in *A* revealed that exon 14 of *EML4* (*blue*) was connected to an 11-bp cDNA fragment of unknown identity (*black*), which was ligated in turn to the nucleotide at position 50 of exon 20 of *ALK* (*red*). *C*, RT-PCR amplification of the fusion point of *EML4-ALK* variant 5 mRNA in NSCLC specimen ID no. 8993 as well as in peripheral blood mononuclear cells of a female volunteer (46,XX). Two specific products of 415 and 298 bp were obtained, corresponding to variants 5b and 5a, respectively. The left lane contains DNA size standards (50-bp ladder). *D*, nucleotide sequencing of the PCR products in *C* revealed that exon 2 of *EML4* was fused either to exon 20 of *ALK*, generating the variant 5a cDNA, or to a position 117 bp upstream of exon 20 of *ALK*, generating the variant 5b cDNA.

Virtual gel electrophoresis of the multiplex RT-PCR products (Fig. 1B) revealed that 11 samples (4.35%) were positive for *EML4-ALK* cDNA among a consecutive series of 253 lung adenocarcinoma specimens, including those examined in our previous studies (8, 9, 13). All of the specimens previously shown to harbor *EML4-ALK* (two cases with variant 1, three with variant 2, and two with variant 3) were faithfully detected with our multiplex RT-PCR system. No specific PCR products were obtained for other types of lung cancer (n = 111) or other solid tumors (n = 292). Nucleotide sequencing of the PCR products for the newly identified positive cases revealed that one specimen was positive for variant 1 and another for variant 3 of *EML4-ALK*, but that the remaining two specimens harbored previously unidentified variants (Fig. 1B and C). Exon 14 of *EML4* was ligated to a position within exon 20 of *ALK* in the product from tumor ID no. 8398 (designated variant 4), whereas exon 2 of *EML4* was ligated to exon 20 of *ALK* in the product from tumor ID no. 8993 (designated variant 5).

Structure of EML4-ALK variant 4 cDNA. To verify the presence of novel *EML4-ALK* variants in the cancer cells, we first did direct RT-PCR analysis for the cDNA of tumor ID no. 8398 with a new set of primers encompassing the putative fusion point of variant 4. This analysis showed the presence of the fusion cDNA (Fig. 2A). Nucleotide sequencing of the PCR product revealed that exon 14 of *EML4* was fused to an unknown sequence of 11 bp, which in turn was connected to the nucleotide at position 50 of exon 20 of *ALK* (Fig. 2B). (We failed to detect a region of the human genome (build 36) homologous to the 11-bp connecting sequence in a BLAST search.[7]) Although exon 14 of *EML4* is not expected to produce an in-frame fusion to exon 20 of *ALK*, insertion of the unknown 11-bp sequence and its ligation to a position within the *ALK* exon allows an in-frame connection between the two genes. Fusion cDNAs in which the point of connection is located within, rather that at the 5′ terminus of, exon 20 of *ALK* have also been described for *MSN-ALK* (14) and *MYH9-ALK* (15).

We further examined whether a full-length cDNA encoding such an unexpected EML4-ALK variant could be isolated from the cancer cells. For this purpose, we designed a sense primer targeted to the 5′ untranslated region of *EML4* cDNA as well as an antisense primer targeted to the 3′ untranslated region of *ALK* cDNA. Direct RT-PCR analysis with this primer set yielded a single PCR product of ~3.4 kbp with total cDNA of tumor ID no. 8398 (Supplementary Fig. S1A). Complete nucleotide sequencing of the PCR product revealed that the cDNA contained an open reading frame for 1,097 amino acids comprising residues 1 to 547 of human EML4, residues 1,075 to 1,620 of human ALK, and 4 amino acids of unknown origin between these two sequences (Supplementary Fig. S1B). The isolation of a full-length cDNA containing the 11-bp insert indicated that the variant 4 protein was likely expressed in the cancer cells.

Structure of EML4-ALK variant 5 cDNAs. We similarly investigated the presence of variant 5 mRNA in the cells of tumor ID no. 8993. Direct RT-PCR analysis to amplify the fusion point of this variant cDNA yielded two independent products of 298 and 415 bp (Fig. 2C). Nucleotide sequencing of each product revealed that the former contained exon 2 of *EML4* and exon 20 of *ALK*, as expected, whereas in the latter, exon 2 of *EML4* was connected to a position within intron 19 of *ALK* located 117 bp upstream of exon 20 (Fig. 2D). These fusion constructs were designated variants 5a and 5b, respectively.

Although no mRNAs or expressed sequence tags in the nucleotide sequence database were found to contain the

[7] http://www.ncbi.nlm.nih.gov/genome/seq/blastgen/blastgen.cgi?taxid=9606

117-bp sequence of intron 19 of *ALK*, the human genome sequence surrounding the 5′ terminus of this 117-bp sequence is AG-GT (Fig. 2D), which conforms to the consensus sequence for a splicing acceptor site. To show that such a cryptic exon is indeed involved in the production of an oncogenic kinase, we attempted to detect full-length cDNAs for variants 5a and 5b from total cDNA of tumor ID no. 8993. A doublet of PCR products of ~2.0 kbp was obtained (Supplementary Fig. S1A), and nucleotide sequencing of these products revealed that they indeed encode EML4-ALK variant 5a and 5b proteins (Supplementary Fig. S1C). Genomic PCR and fluorescence *in situ* hybridization (FISH) analyses further revealed that the cells of tumor ID no. 8993 harbor a single *EML4-ALK* fusion gene, suggesting that variant 5a and 5b mRNAs are generated by alternative splicing of the primary transcript of this single fusion gene (see below).

Detection of the EML4-ALK fusion genes by FISH. To confirm the rearrangements involving the *ALK* locus in the specimens harboring variants 4 and 5 of *EML4-ALK* cDNA, we did FISH analysis with tissue sections. We first designed a FISH-based "fusion assay" for *EML4* and *ALK* genes. Bacterial artificial chromosome fragments encompassing the entire genes were fluorescently labeled green and red, respectively. An overlapping signal for both probes was readily identified in a merged image for the tumor cells harboring variants 4 or 5 of *EML4-ALK* (Fig. 3A). To confirm further the breakage of the *ALK* locus, we did an "*ALK* split assay" with bacterial artificial chromosome fragments encompassing the 5′ or 3′ regions of the locus and labeled green and red, respectively. In this assay, the normal *ALK* locus would be expected to yield an overlapping signal, whereas a pair of separate green and red signals would indicate genomic breakage within *ALK*. As expected, a proportion of cells of tumor ID no. 8398 or no. 8993 in the histologic sections generated one overlapping signal and one pair of split signals (Fig. 3B), suggesting that these tumor cells each have at least one normal and at least one rearranged *ALK* locus.

These data, together with genomic PCR analysis (data not shown), thus indicated that the cells of each of these tumors harbor one normal chromosome 2 and a chromosome 2 with an inv(2)(p21p23) rearrangement. The other *EML4-ALK* cDNA-positive specimens (variants 1 to 3) in this cohort showed a similar FISH labeling profile, consistent with the presence of the corresponding *EML4-ALK* rearrangements (data not shown).

***Detection of EML4-ALK proteins* in situ.** To detect EML4-ALK proteins in the cancer cells, we did immunohistochemical analysis with the ALK1 monoclonal antibody to ALK (16). The cytoplasm of tumor cells harboring *EML4-ALK* variant 1 (ID no. 9034), variant 4 (ID no. 8398), or variant 5 (ID no. 8993) manifested a diffuse pattern of immunoreactivity with fine granular concentrations (Fig. 3C). No normal pulmonary epithelial cells or lymphocytes in the sections of these specimens reacted with the antibody.

Transforming activity of EML4-ALK variants. We prepared expression plasmids for FLAG epitope-tagged EML4-ALK variants 1, 2, 3a, 3b, 4, 5a, and 5b, the predicted molecular sizes of which are 118,356; 146,913; 87,613; 88,874; 122,541; 71,046; and 74,867 Da, respectively. Each of these proteins, as well as a kinase-inactive mutant of EML4-ALK variant 1 (8), was expressed independently in HEK293 cells, immunoprecipitated, and subjected to immunoblot analysis with antibodies to FLAG. Each cDNA generated an EML4-ALK protein of the expected molecular size (Fig. 4A). The same immunoprecipitates were subjected to an *in vitro* kinase assay with the synthetic peptide YFF (12). Each variant protein (with the exception of the kinase-inactive mutant of variant 1) was shown to possess protein tyrosine kinase activity, with that of variants 3a, 3b, and 5b being most prominent (Fig. 4A).

To examine the transforming potential of the EML4-ALK variants, we transfected mouse 3T3 fibroblasts with the corresponding expression plasmids and then cultured the cells for 12 days. Transformed foci were readily detected for the cells expressing the variants of EML4-ALK but not for cells overexpressing wild-type ALK (Fig. 4B). Furthermore, s.c. injection of the transfected 3T3 cells into the shoulder of nude mice revealed that those expressing the various EML4-ALK isoforms, but not those overexpressing wild-type ALK, formed large tumors *in vivo* (Fig. 4B).

Discussion

We have done multiplex RT-PCR analysis to detect all possible isoforms of *EML4-ALK* transcripts in NSCLC cells, and unexpectedly identified two novel subtypes of the fusion event. This finding was supported by detection of the corresponding fusion genes by genomic PCR and FISH

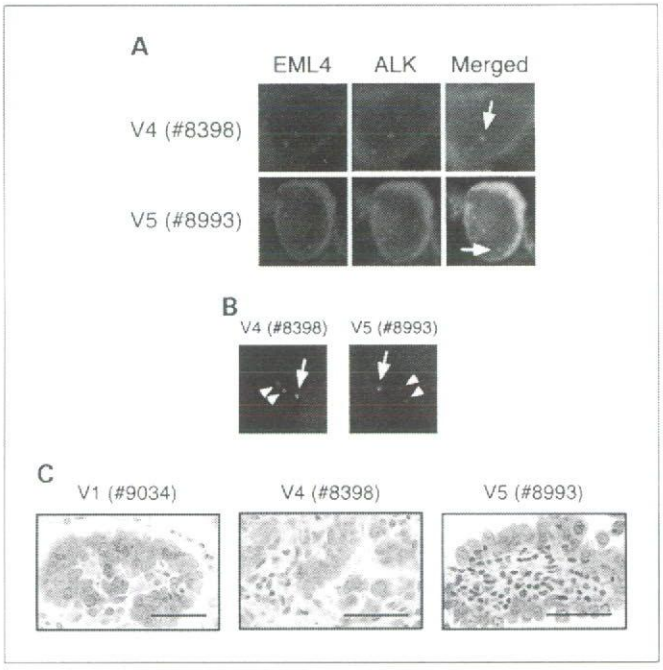

Fig. 3. FISH and immunohistochemical analyses of NSCLC specimens. *A*, FISH analysis of representative cancer cells in sections of lung adenocarcinoma harboring *EML4-ALK* variant 4 (ID no. 8398) or variant 5 (ID no. 8993). Each section was subjected to hybridization with differentially labeled probes for *EML4* (*left*) or for *ALK* (*center*). A fusion signal (*arrow*) and a pair of green (*EML4*) and red (*ALK*) signals are present in each merged image (*right*). *B*, the same clinical specimens as in *A* were subjected to FISH analysis with differentially labeled probes for the 5′ (*green*) or 3′ (*red*) regions of the *ALK* locus. A pair of split signals (*arrowheads*) and an overlapping signal (*arrow*) indicate the rearranged and normal *ALK* loci, respectively. *C*, immunohistochemical analysis of NSCLC specimens positive for *EML4-ALK* variants 1 (ID no. 9034), 4 (ID no. 8398), or 5 (ID no. 8993) with a monoclonal antibody to ALK. A pattern of diffuse staining with fine granular foci was apparent in the cytoplasm of all three tumors. Scale bars, 50 μm.

analyses and by that of the encoded proteins by immunohistochemical analysis in the NSCLC cells. Together with the previously isolated variants (8, 9), we have to date identified a total of seven distinct isoforms of EML4-ALK (variants 1, 2, 3a, 3b, 4, 5a, and 5b). Given that each of these isoforms possesses marked transforming activity, they all likely play an important role in the development of NSCLC. Our failure to detect *EML4-ALK* cDNA in the other solid tumors (n = 313) examined suggests that *EML4-ALK* may be an oncogene specific to NSCLC, especially to lung adenocarcinoma.

In our multiplex RT-PCR analysis, a sense primer targeted to exon 2 of *EML4* was designed to detect fusion events involving exon 2 or 6 of *EML4*, and PCR products of the expected sizes were indeed obtained with NSCLC specimens positive for such fusion events (variants 5 and 3, respectively). The other sense primer was targeted to exon 13 of *EML4* and was designed to detect fusion events involving exon 13, 18, 20, or 21 of *EML4*. Given that we were able to readily amplify a specific product of 1185 bp corresponding to the fusion event involving exon 20 of *EML4* (variant 2), it is likely that all possible fusions giving rise to PCR products up to this size would have been detected in our cohort. It should be noted, however, that a possible fusion between exon 21 of *EML4* and exon 20 of *ALK* would be expected to generate a PCR product of 1,284 bp. Although the size difference between the 1,185- and 1,284-bp products is small (99 bp), it is still possible that our multiplex RT-PCR analysis failed to efficiently amplify the longer product and that there may be as-yet-undetected fusion events for *EML4-ALK* in our cohort.

All EML4-ALK isoforms manifested a similar subcellular distribution profile despite marked differences in the size and domain structure of the EML4 portions of these chimeric proteins. In addition, the intracellular signaling systems activated by EML4-ALK may be shared among variants 1 to 5 (Supplementary Fig. S2). The EML4 portion of variant 5 comprises only the coiled-coil domain. This domain of EML4 may therefore play an essential role not only in the dimerization and activation of EML4-ALK isoforms (8) but also in tethering EML4-ALK to specific subcellular components. The pattern of subcellular immunostaining for EML4-ALK (cytoplasmic staining with fine granular foci) was distinct from that for other ALK fusion proteins associated with other malignancies (17, 18), suggesting that the subcellular localization of ALK fusion kinases varies substantially. The first such fusion kinase to be identified, NPM-ALK, preferentially phosphorylates STAT3, which is thought to participate in mitogenic signaling by NPM-ALK (19–21). Five ALK fusion kinases (NPM-ALK, TFG-ALK, ATIC-ALK, TPM3-ALK, and CLTC-ALK) were shown to differ markedly in their abilities to transform 3T3 fibroblasts, to phosphorylate STAT3 and AKT, and to activate phosphoinositide 3-kinase (17). Furthermore, a proteomics approach to identify tyrosine-phosphorylated proteins failed to detect marked phosphorylation of STAT3 in NSCLC specimens positive for EML4-ALK (22). It is therefore likely that each ALK fusion kinase exerts its effects through fusion-specific (although possibly partially overlapping) downstream pathways. In addition, we detected slight differences in catalytic and transforming activities among the variants of EML4-ALK (Fig. 4). These differences are likely due to the different portions of EML4 present in the different variants, which may affect dimerization affinity or the recruitment of substrates.

In addition to *EML4-ALK*, NSCLC cells harbor other potent oncogenes such as mutant versions of *EGFR* or *KRAS*. These three oncogenes, however, were found to be mutually exclusive

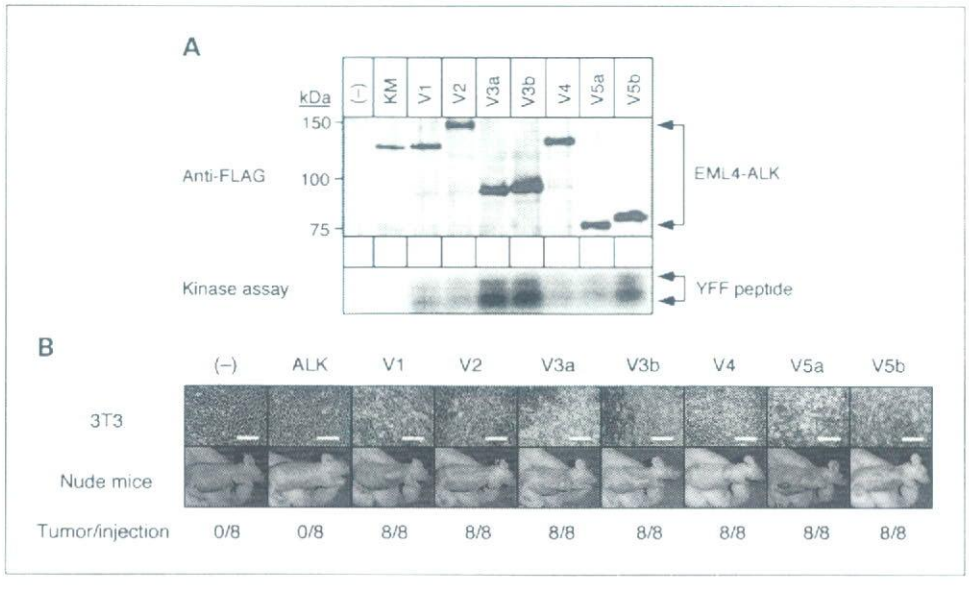

Fig. 4. Transforming potential of EML4-ALK variants. *A*, HEK293 cells expressing FLAG-tagged variant 1, 2, 3a, 3b, 4, 5a, or 5b of EML4-ALK were lysed and subjected to immunoprecipitation with antibodies to FLAG. The resulting precipitates were then either subjected to immunoblot analysis with antibodies to FLAG (*top*) or assayed for kinase activity with the synthetic YFF peptide (*bottom*). Cells transfected with the empty vector (-) or with a vector for a kinase-inactive mutant (*KM*) of EML4-ALK variant 1 were also analyzed. The positions of molecular size standards (kDa) and of EML4-ALK proteins are indicated on the left and right of the top panel, respectively. *B*, mouse 3T3 fibroblasts were transfected with expression plasmids for wild-type ALK or FLAG-tagged EML4-ALK variants, or with the empty plasmid (-), and were photographed after culture for 12 d (*top*). Scale bars, 200 μm. Alternatively, the transfected cells were injected s.c. into the shoulder of nu/nu mice and tumor formation was examined after 20 d (*bottom*). The number of tumors formed per eight injections is indicated at the bottom.

in our previous NSCLC cohort (8, 13), suggesting that EML4-ALK–positive NSCLC is a distinct subclass of lung cancer. Given that a selective inhibitor of the kinase activity of ALK rapidly induces cell death in EML4-ALK–positive cancer cells both *in vitro* (8, 9) and *in vivo*,[8] determination of the presence or absence of *EML4-ALK* in a given tumor may in the future inform the choice of treatment strategy for NSCLC. The demonstration of the existence of multiple isoforms of *EML4-ALK* transcripts will necessitate optimization of the detection systems so that all isoforms are detected with a high accuracy and sensitivity.

[8] M. Soda et al., submitted for publication.

Note Added in Proof

During our revision process, a novel EML4-ALK fusion variant was reported by Koivunen et al. (Clin Cancer Res 2008;14:4275–83). They have designated it as variant 4, which is different from our variant 4 in the present study.

Disclosure of Potential Conflicts of Interest

K. Takeuchi is a consultant providing advisory services to Dako for their antibodies.

Acknowledgments

We thank Kazuko Yokokawa, Motoyoshi Iwakoshi, Miyuki Kogure, and Tomoyo Kakita for technical assistance as well as Yuki Takano for help in preparation of the manuscript.

References

1. Aplan PD. Causes of oncogenic chromosomal translocation. Trends Genet 2006;22:46–55.
2. Sherbenou DW, Druker BJ. Applying the discovery of the Philadelphia chromosome. J Clin Invest 2007;117:2067–74.
3. Pulford K, Morris SW, Turturro F. Anaplastic lymphoma kinase proteins in growth control and cancer. J Cell Physiol 2004;199:330–58.
4. Mitelman F, Johansson B, Mertens F. Fusion genes and rearranged genes as a linear function of chromosome aberrations in cancer. Nat Genet 2004;36:331–4.
5. Mitelman F, Johansson B, Mertens F. The impact of translocations and gene fusions on cancer causation. Nat Rev Cancer 2007;7:233–45.
6. Tomlins SA, Rhodes DR, Perner S, et al. Recurrent fusion of TMPRSS2 and ETS transcription factor genes in prostate cancer. Science 2005;310:644–8.
7. Tomlins SA, Laxman B, Dhanasekaran SM, et al. Distinct classes of chromosomal rearrangements create oncogenic ETS gene fusions in prostate cancer. Nature 2007;448:595–9.
8. Soda M, Choi YL, Enomoto M, et al. Identification of the transforming EML4-ALK fusion gene in non-small-cell lung cancer. Nature 2007;448:561–6.
9. Choi YL, Takeuchi K, Soda M, et al. Identification of novel isoforms of the EML4-ALK transforming gene in non-small cell lung cancer. Cancer Res. In press 2008;68:4971–6.
10. Travis WD, Elisabeth B, Muller-Hermelink HK, Harris CC, editors. Pathology and genetics of tumours of the lung, pleura, thymus and heart. Lyon: IARC Press; 2004.
11. Onishi M, Kinoshita S, Morikawa Y, et al. Applications of retrovirus-mediated expression cloning. Exp Hematol 1996;24:324–9.
12. Donella-Deana A, Marin O, Cesaro L, et al. Unique substrate specificity of anaplastic lymphoma kinase (ALK): development of phosphoacceptor peptides for the assay of ALK activity. Biochemistry 2005;44:8533–42.
13. Inamura K, Takeuchi K, Togashi Y, et al. EML4-ALK fusion is linked to histological characteristics in a subset of lung cancers. J Thorac Oncol 2008;3:13–7.
14. Tort F, Pinyol M, Pulford K, et al. Molecular characterization of a new ALK translocation involving moesin (MSN-ALK) in anaplastic large cell lymphoma. Lab Invest 2001;81:419–26.
15. Lamant L, Gascoyne RD, Duplantier MM, et al. Non-muscle myosin heavy chain (MYH9): a new partner fused to ALK in anaplastic large cell lymphoma. Genes Chromosomes Cancer 2003;37:427–32.
16. Pulford K, Lamant L, Morris SW, et al. Detection of anaplastic lymphoma kinase (ALK) and nucleolar protein nucleophosmin (NPM)-ALK proteins in normal and neoplastic cells with the monoclonal antibody ALK1. Blood 1997;89:1394–404.
17. Armstrong F, Duplantier MM, Trempat P, et al. Differential effects of X-ALK fusion proteins on proliferation, transformation, and invasion properties of NIH3T3 cells. Oncogene 2004;23:6071–82.
18. Duyster J, Bai RY, Morris SW. Translocations involving anaplastic lymphoma kinase (ALK). Oncogene 2001;20:5623–37.
19. Wan W, Albom MS, Lu L, et al. Anaplastic lymphoma kinase activity is essential for the proliferation and survival of anaplastic large-cell lymphoma cells. Blood 2006;107:1617–23.
20. Marzec M, Kasprzycka M, Ptasznik A, et al. Inhibition of ALK enzymatic activity in T-cell lymphoma cells induces apoptosis and suppresses proliferation and STAT3 phosphorylation independently of Jak3. Lab Invest 2005;85:1544–54.
21. Galkin AV, Melnick JS, Kim S, et al. Identification of NVP-TAE684, a potent, selective, and efficacious inhibitor of NPM-ALK. Proc Natl Acad Sci U S A 2007;104:270–5.
22. Rikova K, Guo A, Zeng Q, et al. Global survey of phosphotyrosine signaling identifies oncogenic kinases in lung cancer. Cell 2007;131:1190–203.

Pulmonary Ground-Glass Opacity (GGO) Lesions–Large Size and a History of Lung Cancer are Risk Factors for Growth

Miyako Hiramatsu, MD,† Takuya Inagaki, MD,* Tomoya Inagaki, MD,* Yoshio Matsui, MD,* Yukitoshi Satoh, MD, PhD,* Sakae Okumura, MD,* Yuichi Ishikawa, MD, PhD,‡ Etsuo Miyaoka, PhD,§ and Ken Nakagawa, MD**

Objective: Ground-glass opacity (GGO) of the lung is being frequently detected by thin section computed tomography scan. However, the long term management of detected GGO is still unclear. To establish follow-up plans, we performed the clinical and radiological review to identify the factors that are closely associated with GGO growth.

Methods: We retrospectively analyzed computed tomography images of 125 GGOs that were stable for 3 months between 1999 and 2006 at the Cancer Institute Hospital, Tokyo. To identify factors that affect the roentgenological growth, the time to GGO growth curve by Kaplan-Meyer method was evaluated in terms of gender, age, smoking, initial size, existence of a solid part, GGO density, location, multiplicity, and lung cancer history by univariate and multivariate analyses.

Results: The median observation period was 1048 days (177–3269) and 26 of 125 GGOs (21%) grew. The estimated growth population for 5 years was 30%. The growth was more frequently seen in the elderly ($p = 0.017$), in part-solid GGO ($p < 0.01$) and in GGO of larger than 10 mm ($p < 0.01$, logrank test). By multivariate analysis, initial size ($p < 0.01$, Cox's model) and history of lung cancer ($p = 0.017$, logistic model) were independent factors that were significantly associated with GGO growth. Fifty GGOs that were 10 mm or smaller and without a lung cancer history did not grow within 3.5 years.

Conclusions: After initial management and 3 month follow-up, larger size (more than 10 mm) and a history of lung cancer are risk factors for GGO growth, and therefore should be considered when making a follow-up plan.

Key Words: Lung Adenocarcinoma, Ground-glass, Follow-up, Thin-section CT.

(*J Thorac Oncol.* 2008;3: 1245–1250)

Recent studies have demonstrated that screening with low-dose computed tomography (CT) can improve detection of lung cancer at an early and potentially curable stage.[1,2] Since CT screening has become more widely accepted and with advances in technique, very faint and smaller lesions called ground-glass opacities (GGOs) are now frequently encountered. GGO is a roentgenological term for lesions in the lung on thin section CT (TSCT), defined as a homogeneous hazy increase in density in the lung field that does not obscure the bronchiolovascular structure.[3,4] Recently GGOs were found in 0.2 to 0.5% of screened populations.[5] Pathologically, localized GGOs existing for months have been reported to correspond to precancerous lesions or early stage adenocarcinomas.[6–10] These pathologic conditions include atypical adenomatous hyperplasia (AAH) and bronchioloalveolar carcinoma (BAC) which replace alveolar epithelial cells according to the World Health Organization definition.[11] Although GGOs are generally reported to grow slowly, details of natural history remain limited.[12,13]

In this study, we therefore examined GGOs and part-solid GGOs that existed for more than 3 months on chest TSCT in our hospital. The purpose was to clarify factors that are likely to affect the growth of a GGO and to gain a better understanding to facilitate appropriate GGO follow-up planning.

PATIENTS AND METHODS

Patients

Between 1999 and 2006, 184 patients were referred to the Department of Thoracic Surgical Oncology, the Cancer Institute Hospital, Tokyo, for further examination of lung lesions that seemed as a GGO on chest TSCT. Among these, 17 patients (9%) had an immediate diagnostic work-up including surgical intervention and 10 patients were lost to

*Department of Thoracic Surgical Oncology, the Cancer Institute Hospital of the Japanese Foundation for Cancer Research (JFCR), Koto-ku, Tokyo, Japan; †Department of Surgery, Tokyo Jikei University School of Medicine, Tokyo, Japan; ‡Department of Pathology, the Cancer Institute of the Japanese Foundation for Cancer Research (JFCR), Koto-ku, Tokyo, Japan; and §Department of Mathematics, Tokyo University of Science, Tokyo, Japan.

Supported by Grants-in-Aid for Scientific Research from the Ministry of Education, Culture, Sports, Science and Technology, from the Japan Society for the Promotion of Science, and by grants from the Ministry of Health, Labour and Welfare, the Smoking Research Foundation, and the Vehicle Racing Commemorative Foundation.

Disclosure: The authors declare no conflicts of interest.

Address for correspondence: Ken Nakagawa, MD, Department of Thoracic Surgical Oncology, the Cancer Institute Hospital of the JFCR, 3-10-6 Ariake, Koto-ku, Tokyo 135-8550, Japan. E-mail: knakagawa@jfcr.or.jp

ISSN: 1556-0864/08/0311-1245

follow-up. Although the remaining 157 patients were then followed-up for 3 months by CT scan, it was terminated in 32 patients for the following reasons (number of patients); vanished, (6) gross growth, (3) rapid increase in number and recognition as pulmonary metastasis, (4) advance in other malignancy, (1) patient's request, (3) and lost to follow-up. (11) TSCT was repeated and 125 patients, who showed no change in the repeat CT images, were finally enrolled in the study. Their clinicopathologic background and CT findings are shown in Table 1. Although 45 patients (36%) had multiple GGOs (range of number, 2–20), we only considered the largest lesions. Follow-up consisted of periodic TSCT at a 6-month intervals. The mean observation period was 1048 days (ranged, 177–3269), and follow-up CT scans were performed an average of 6 times in each case. In 59 cases, GGOs were detected at a health check-up or were found incidentally, and the others were detected during follow-up of prior malignancy (51 patients with lung adenocarcinoma (stage I, 48; stage II, 1; stage III, 2), 9 with breast cancer, 2 with gynecologic cancer, 2 with urologic cancer, and 2 with sarcomas). Nine patients with a history of lung cancer also had other cancers in other organs. The interval between the prior malignancy treatment and detection of the current GGO varied from 0 to 168 (mean 36) months among these 66 patients.

TABLE 1. Patient Background and CT Findings

	Total $n = 125$	With Growth $n = 26$ (%)
Patient background		
Gender		
Men	51	13 (25)
Women	74	13 (18)
Age (36–88, mean 62)		
≤60	44	5 (11)
60<	81	21 (26)
Smoking habit		
Never	58	10 (17)
Ever	41	10 (24)
Unknown	26	6 (23)
History of lung cancer		
Without	74	11 (15)
With	51	15 (29)
CT findings		
Initial size (3–17 mm, mean 8.3)		
≤10	87	8 (9)
10<	38	18 (47)
Existence of solid part		
Without (GGO)	95	14 (15)
With (part-solid GGO)	30	12 (40)
CT density (−810 to −10 HU)[a]		
≤−500	67	10 (15)
−500<	58	16 (28)
Location[b]		
Above	79	19 (24)
Below	46	7 (15)
Multiplicity		
Solitary	80	17 (21)
Multiple	45	9 (20)

[a] The mean CT density (HU) of 3 spots within the GGO.
[b] With reference to the major fissure of the lung.
GGO, ground-glass opacity; CT, computed tomography.

This retrospective study was approved by the institutional review board of the Cancer Institute Hospital of the Japanese Foundation for Cancer Research.

Radiologic Definition of GGOs and Their "Growth" on TSCT

CT scan was performed with a GE Yokogawa Medical System, Light Speed QXi or High Speed DXi (Hino, Tokyo). For screening of the whole lung field, the scanning parameters were as follows: 120 kV, 230 mA, beam width of 7.5 mm, rotation speed of 1 revolution/s, table speed of 15 mm/s (pitch 2:1), and a reconstruction interval of 7.5 mm. When the presence of GGO was suspected, targeted axial scanning was repeated only for the suspected area based on the previous scanning. The scanning parameters were 120 kV, 280 mA (or 180 mA), clustered axial scanning of 1.25 mm or 2.0 mm slice and the largest diameter of the lesion was evaluated at WL-585HU and WW1800HU.[14] All scans were obtained in full inspiration without any contrast material and viewed in cine format on a computer workstation. All radiologic images were evaluated by 2 of the specialists who had 5 and 17 years of experience (MH, YS), respectively and a final consensus was obtained by plenary reading. The size of each lesion was recorded by evaluating the largest diameter using a caliper tool in the software. In this study, we discriminate "part-solid GGO" from "GGO." The definition of them was based on that of Henschke et al.,[15] in which the subcategories "nonsolid" and "part-solid" were recognized according to the absence/presence of solid parts in the GGO lesion. We prefer the term "GGO" to "nonsolid nodule" because a finding of GGO on TSCT corresponds specifically to a pathologic alveolar condition with noninvasive tumor-spreading, while "nonsolid nodule" does not. The remainder (24%) had a solid part, the diameter of which as a proportion of the diameter of the whole lesion was (solid part/ GGO) from 0.13 to 0.42 (2/16 mm–2.5/6 mm) and we used the term "part-solid GGO" for them in this study. All GGOs with extra findings (6 GGOs with cystic components and 12 GGOs with heterogeneous ground-glass density) were included as "GGO." The "CT density" was defined as the mean density (HU) measured at three spots within the GGO part of each lesion with the software tool. "Growth" of a GGO was concluded when any of the following were recognized: gross increase in the greatest dimension by at least 2 mm from the initial TSCT (Figure 1), gross increase in the size of the solid part by at least 2 mm, or a new solid part of any size (Figure 2).

Statistical Analysis

The follow-up time was defined from the date of the initial TSCT to the latest TSCT. To clarify the factors that may affect GGO growth, univariate and multivariate analyses were performed with regard to the growth incidence (numbers of GGO with concluded growth/numbers at risk). In this retrospective investigation, multivariate analyses were ap-

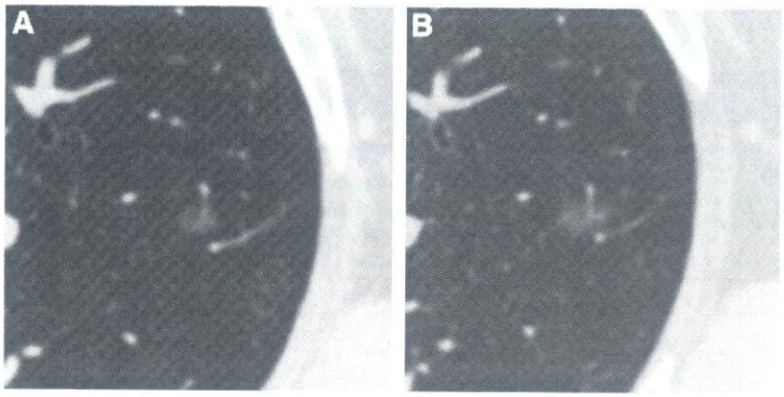

FIGURE 1. A case showing GGO increase in size. (*A*) GGO in the left upper lobe, measuring 7 mm in diameter at detection. (*B*) Growth by 3 mm was confirmed after 10 months.

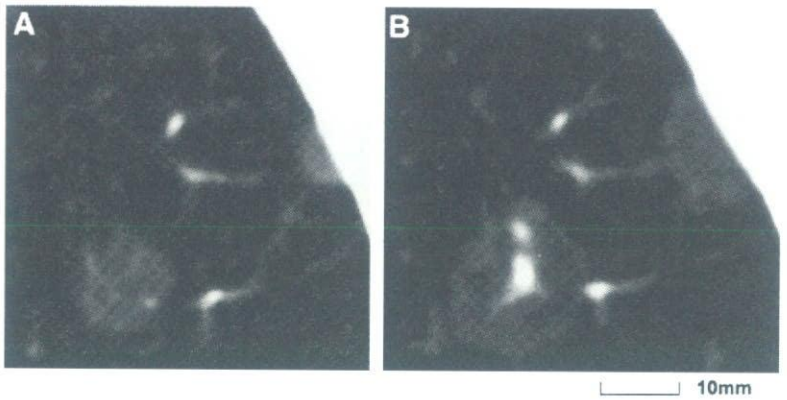

FIGURE 2. A case with GGO increase in size and formation of a solid part. (*A*) 9 mm and 7 mm GGOs detected in the left upper lobe. (*B*) Growth in size (to 17 and 12 mm, respectively) and became part-solid GGO after 7 months.

plied for two separate studies: one to evaluate the time to GGO growth and the other to evaluate GGO growth incidence. For the first, the time to GGO growth curves were estimated by the Kaplan-Meier method, and the difference of the time to GGO growth curve between each group was tested by the log-rank test. Independent variables that influenced the time to GGO growth were analyzed by Cox's proportional hazard model. For the analysis, the original continuous variables, such as age, CT density (HU), and initial size, were dichotomized at clinically appropriate cutoff values (60 years, −500 HU and 10 mm, respectively). In the second study, a logistic-regression analysis was performed to clarify variables that affected GGO growth incidence. Finally, variables were selected by multivariate matched sampling methods in both studies.

RESULTS

Characteristics of GGOs with Growth

The clinical and radiologic characteristics of all cases were presented in Table 1. Among 125 patients with GGOs who underwent repeated TSCT for 3 months or more, 26 patients (21%) had overt GGO growth which met our definitions. With 13 GGOs (10%), enlargement of the greatest dimension was documented. These lesions consisted of 8 GGOs of 5 to 13 mm and 5 part-solid GGOs of 8 to 16 mm, and 2 of each had a history of lung cancer. An increase in both the greatest dimension and the size of the solid part was evident in 7 part-solid GGOs (6%) of 11 to 17 mm. Six GGOs measuring 8 to 16 mm became part-solid GGOs (5%).

The histopathological features were studied in 9 GGOs with growth. Specimens were obtained by surgical exploration in 7 (5 with lobectomy and 2 with segmentectomy), and by fine needle aspiration and by transbronchial lung biopsy in one each. The histologic diagnosis was made according to the World Health Organization classification[11]: adenocarcinoma with mixed subtype was seen in 6, nonmucinous BAC in 2, and organizing pneumonia in one. Of these 9 GGOs that underwent evaluation, 6 were detected at a health check-up and the rest were detected more than 2 years after an operation for stage I lung cancer. In contrast, 9 of the remaining 17 cases with growing GGOs had advanced tumors. Further evaluation was applied mainly depending on the background and the patient's request, particularly in the earlier period because the natural history of GGO had not yet been well described. No metastasis or tumor-related deaths were observed clinically.

Time to GGO Growth Curves and Univariate Analysis for Factors that Affect the Time to GGO Growth

The time to GGO growth curve for 125 GGOs is shown in Figure 3. Growth incidence at 3 and 5 years were estimated

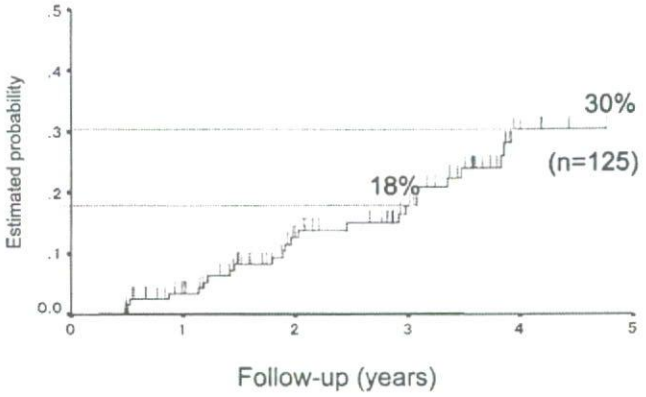

FIGURE 3. The time to GGO growth curve for the 125 GGOs. The growth incidence at 5 years was estimated to be 30% in this study.

TABLE 2. Univariate Analysis for Factors Affecting the Time to GGO Growth

Variables	Estimated Probability 3 yr	Estimated Probability 5 yr	p
Gender			0.15
Men	0.26	0.39	
Women	0.13	0.25	
Age			0.017
≤60	0.09	0.13	
60<	0.23	0.41	
Smoking habit			0.16
Never	0.09	0.23	
Ever	0.29	0.41	
History of lung cancer			0.22
With	0.19	0.22	
Without	0.16	0.38	
Initial size			<0.01
≤10	0.04	0.14	
10<	0.49	0.66	
Existence of solid part			<0.01
Without (GGO)	0.12	0.18	
With (part-solid GGO)	0.43	0.80	
CT density (HU)			0.17
≤−500	0.16	0.20	
−500<	0.20	0.40	
Location[a]			0.78
Above	0•19	0.31	
Below	0.13	0.28	
Multiplicity			0.60
Solitary	0.22	0.35	
Multiple	0.10	0.23	

[a] With reference to the major fissure of the lung.
GGO, ground-glass opacity; CT, computed tomography.

to be 18% and 30%, respectively, with no plateau. Statistically significant influence on time to growth was evident for age ($p = 0.017$), existence of solid part ($p < 0.01$) and initial size ($p < 0.01$). With regard to the initial size of GGO, we determined an appropriate cutoff size by using the time to GGO growth curve and found that 2 curves were maximally distinguished with an initial size of 10 mm. However, no differences in the time to GGO growth were observed according to such clinical factors as gender, smoking habit, history of lung cancer, or radiologic findings like size, existence of solid part, CT density, location, or multiplicity (Table 2). The time to GGO growth curves with reference to initial sizes (10 mm or smaller and larger than 10 mm) are shown in Figure 4 and the growth incidence of each group at 5 years were estimated to be 14% and 66%, respectively, the difference being statistically significant ($p < 0.01$).

Multivariate Analyses for Factors that Affect GGO Growth

The results of the multivariate analysis by Cox's proportional hazard model are shown in Table 3. Only initial size was significantly associated with the time to GGO growth ($p < 0.01$). In contrast, both the initial size ($p = 0.018$) and

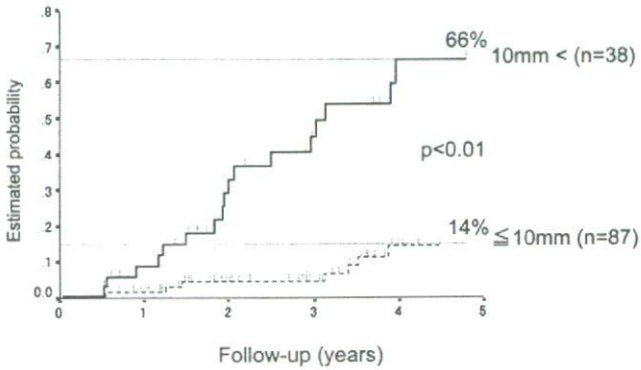

FIGURE 4. The time to GGO growth curves according to initial size of GGO. The growth incidence for 10 mm or smaller ($n = 87$) and larger ($n = 38$) at 5 years were 14% and 66%, respectively. The difference between the curves was statistically significant ($p < 0.01$).

TABLE 3. Multivariate Analysis for Factors Affecting the Time to GGO Growth by Cox Proportional Hazard Model

	SD	HR	95% CI	p
Gender	0.55	0.71	0.24–2.11	0.54
Age	0.028	1.00	0.95–1.06	0.79
History of lung cancer	0.61	2.15	0.65–7.15	0.21
Smoking habit	0.60	1.54	0.47–5.12	0.68
Initial size	0.085	1.28	1.08–1.51	<0.01
Existence of solid part	0.76	1.66	0.37–7.37	0.51
CT density (HU)	0.002	1.00	0.99–1.00	0.89
Location	0.56	0.86	0.29–2.57	0.79
Multiplicity	0.55	0.63	0.21–1.85	0.40
Final model				
Initial size	0.06	1.36	1.21–1.53	<0.01

GGO, ground-glass opacity; SD, standard deviation; HR, hazard ratio; CI, confident interval.

TABLE 4. Multivariate Analysis for Factors Affecting the Time to GGO Growth by Logistic Regression

	SD	OR	95% CI	p
Gender	0.78	0.47	0.10–2.16	0.33
Age	0.035	0.99	0.93–1.07	0.95
History of lung cancer	0.74	4.80	1.13–20.33	0.033
Smoking habit	0.76	0.91	0.21–4.03	0.91
Initial size	0.11	1.29	1.05–1.60	0.018
Existence of solid part	0.80	1.84	0.39–8.75	0.44
CT density (HU)	0.002	1.00	0.99–1.005	0.70
Location	0.67	0.62	0.17–2.29	0.47
Multiplicity	0.69	0.53	0.14–2.05	0.36
Final model				
Initial size	0.080	1.42	1.21–1.66	<0.01
History of lung cancer	0.53	3.51	1.25–9.88	0.017

GGO, ground-glass opacity; SD, standard deviation; OR, odds ratio; CI, confident interval.

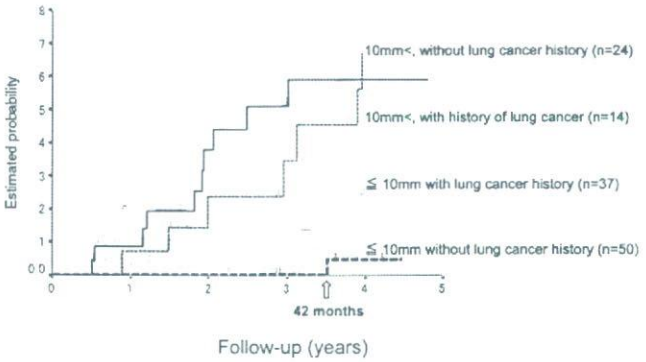

FIGURE 5. The time to GGO growth curve was divided according to the initial size and a history of lung cancer. Fifty GGOs that were 10 mm or less in diameter and without a previous history of lung cancer did not grow within the follow-up period of 42 months.

history of lung cancer ($p = 0.033$) were independent factors that were significantly associated with GGO growth on multivariate analysis of logistic regression (Table 4). The factor "history of lung cancer" seemed to influence the growth incidence after the third year of follow-up and this might be the reason why this parameter became significant only when using the logistic regression model. The time to GGO growth curves according to the initial size and history of lung cancer were shown in Figure 5. The growth population of 50 GGOs that were 10 mm or smaller and without a history of lung cancer stayed 0% until 42 months. However, the growth population of other GGOs started to rise within the first year.

DISCUSSION

Localized GGOs found on high-resolution chest CT scans have been reported to correspond histologically to preinvasive or early stage forms of adenocarcinoma.[6–11] Although the natural history of GGOs is speculated to correspond to progression from AAH to invasive adenocarcinoma, sequential changes are not well detailed. Clinically, localized GGOs are considered to exhibit slow growth.[12] Hasegawa et al. showed that the tumor doubling times of GGOs and solid-type lesions were 813 ± 375 and 149 ± 125 days, respectively.[13] Since biopsy or excision of these lesions in the lung is relatively difficult, these slow growing GGOs are currently considered for follow-up instead of definite diagnosis or treatment.[16,17] However, an appropriate follow-up period and a consensus intervention strategy have yet to be determined.

Recently, a close correlation between the size of resected GGOs and histology was reported. Nakata et al. analyzed GGOs less than 2 cm in diameter and found that the average sizes for AAH, BAC, and adenocarcinoma were 6.8 mm, 10.0, and 12.5 mm, respectively; the difference being statistically significant.[7] According to Takashima et al. lesion size, percentage of GGO area within a lesion, lobulation, coarse spiculation, air bronchogram, cavity, a pleural tag, and a solid portion are related to histopathological diagnosis as AAH, BAC, or adenocarcinoma.[18] Furthermore, the growth fraction of these tumor cells is known to increase according to sequential progression from AAH to BAC then adenocarcinoma.[19] These observations suggested that larger GGOs are more likely to have an invasive character, and therefore a high growth incidence can reasonably be expected for larger GGOs. In the present study, 26 of 125 GGOs (21%) showed obvious growth during the follow-up period, and the initial size of GGO was identified as an independent factor that affected GGO growth incidence and the time to GGO growth on multivariate analyses. In the International Early Lung Cancer Action Project protocol, observation and follow-up CT scan within a few months is recommended for any GGO 8 to 15 mm in diameter.[16] In the present study, the difference in growth population curves for GGOs 10 mm or smaller and GGOs larger than 10 mm was statistically significant. Therefore the interval of follow-up TSCT for each case should be set differently according to the initial size.

Moreover, our multivariate analysis demonstrated that a past history of lung cancer was also an independent factor affecting the growth of GGO. Kodama et al. reported similar observations; 19 GGOs were followed up, and growth was seen in 6 of 7 GGOs with a history of lung cancer but in only 4 of 12 GGOs without such a history.[20] Although the reason for the higher growth incidence in patients with a history of lung cancer is unclear, one possibility is that these newly developing GGOs are intrapulmonary metastases or recurrences. However, none of our 51 patients with a past history of lung cancer developed extrathoracic metastasis or bilateral multiple metastasis during the follow-up period. Therefore, the significant percentage in the present series can not be explained on this basis. Also, in CT images, recurrent intrapulmonary metastases are not likely to present with a GGO appearance.[5,21] Another possibility is that these GGOs are metachronous second primary lesions with a more aggressive nature and a faster speed of growth. In previous reports, the prevalence of second primary lung cancers was reported to be 0.8 to 10.0%, and the 5-year survival rate after the development of metachronous lesion varied from 18 to 39%.[22–26]

However, these reports considered only solid tumors of different histologies and of larger size than recent CT detected tumors, so much better survival is expected for GGOs even with a prior history of lung cancer. Without genetic confirmation, it is difficult to distinguish between metastasis or recurrence and second primary tumor, even with a comparison of histology.[27,28] In the present study, however, it was strongly suggested that the GGOs need to be carefully followed-up in patients with a history of lung cancer.

The timing of terminating the follow-up is another important issue in the management of GGO. In the present study, 50 GGOs that were 10 mm or less in diameter and without a previous history of lung cancer did not grow within the follow-up period of 42 months. Although the number of patients studied here was not large, these data suggested that the interval between the initial CT and the second CT for such GGOs could be extended to at least 3 years. Further accumulation of data is crucial to establish an appropriate follow-up strategy for patients with GGO lesions with varied backgrounds.

In conclusion, independent factors that significantly affect the growth of GGO were initial size, in particular larger than 10 mm, and a history of lung cancer in our series. Therefore, in the follow-up/work-up strategy for GGOs, these two factors should be taken into consideration so as not to overlook aggressive tumors. It is also important to note that these recommendations should be applied only after initial management and a 3-month follow-up have been performed. The possibility of putting-off the follow-up CT for 3 years for a GGO of 10 mm or smaller in a patient without any history of lung cancer should also be explored. In contrast, follow-up CT within a year should be recommended for larger GGOs or GGOs with a history of lung cancer.

ACKNOWLEDGMENTS

We greatly appreciate the technical support of Mr. Tomomasa Terahira at the Cancer Institute Hospital, Tokyo, Japan and the assistance of Drs. Masato Matsushima and Mio Sakuma at the Division of Clinical Research and Development, The Jikei University School of Medicine, with the data analysis.

REFERENCES

1. Henschke CI, McCauley DI, Yankelvitz DF, et al. Early lung cancer action project: overall design and findings from baseline screening. *Lancet* 1999;354:99–105.
2. Sone S, Takashima S, Li F, et al. Mass screening for lung cancer with a mobile spiral computed tomography scanner. *Lancet* 1998;351:1242–1245.
3. Austin JHM, Muller N, Friedman PJ, et al. Glossary of terms for CT of the lungs: recommendations of the Nomenclature Committee of the Fleischner Society. *Radiology* 1996;200:327–331.
4. Collins J, Stern EJ. Ground-glass opacity at CT: The ABCs. *Am J Roentgenol* 1997;169:355–367.
5. Henschke CI, Shaham D, Yankelevitz DF, et al. CT screening for lung cancer: significance of diagnoses in its baseline cycle. *Clin Imaging* 2006;30:11–15.
6. Nakajima R, Yokose T, Kakinuma R, et al. Localized ground-glass opacity on high-resolution CT: histologic characteristics. *J Comput Assist Tomogr* 2002;26:323–329.
7. Nakata M, Saeki H, Takata I, et al. Focal ground-glass opacity detected by low-dose helical CT. *Chest* 2002;121:1464–1467.
8. Jang HJ, Lee KS, Kwon OJ, et al. Bronchioloalveolar carcinoma: focal area of ground-glass attenuation at thin-section CT as an early sign. *Radiology* 1996;199:485–488.
9. Kushihashi T, Munechika H, Ri K, et al. Bronchioloalveolar adenoma of the lung: CT-pathologic correlation. *Radiology* 1994;193:789–793.
10. Zwirewich CV, Vedal S, Miller RR, et al. Solitary pulmonary nodule: high-resolution CT and radiologic-pathologic correlation. *Radiology* 1991;179:469–476.
11. Travis WD, Bambilla E, HK Muller-Hermelink, CC Harris. Pathology and Genetics of Tumours of the Lung, Pleura, Thymus and Heart. Lyon (France): IARC, 2004.
12. Aoki T, Nakata H, Watanabe H, et al. Evolution of peripheral lung adenocarcinomas: CT findings correlated with histology and tumor doubling times. *Am J Roentgenol* 2000;174:763–768.
13. Hasegawa M, Sone S, Takashima S, et al. Growth rate of small lung cancers detected on mass CT screening. *Br J Radiol* 2000;73:1252–1259.
14. Japan Lung Cancer Society, (Eds). General Rule for Clinical and Pathological Record of Lung Cancer. 6th ed. Tokyo: Kanehara Shuppan, 2003 (In Japanese).
15. New York Early Lung Cancer Action Project Investigators. CT screening for lung cancer: diagnosis resulting from the New York Early Lung Cancer Action Project. *Radiology* 2007;243:239–249.
16. New York Early Lung Cancer Action Project [IELCAP Web site]. Available at: http://www.ielcap.orf/ielcap2.pdf. Accessed August 1, 2007.
17. Libby DM, Smith JP, Aktorki NK, et al. Managing the small pulmonary nodule discovered by CT. *Chest* 2007;125:1522–1529.
18. Takashima S, Maruyama Y, Hasegawa M, et al. CT findings and progression of small peripheral lung neoplasms having a replacement growth pattern. *Am J Roentgenol* 2003;180:817–826.
19. Kitamura H, Kameda Y, Nakamura N, et al. Proliferative potential and p53 overexpression in precursor and early stage lesions of bronchioloalveolar lung carcinoma. *Am J Pathol* 1995;146:876–887.
20. Kodama K, Higashiyama M, Yokouchi H, et al. Natural history of pure Ground Glass Opacity after long-term follow-up of more than 2 years. *Ann Thorac Surg* 2002;73:386–393.
21. Ohta R, Yamashita M, Nakata M, et al. Multiple ground-glass opacity in metastasis of malignant melanoma diagnosed by lung biopsy. *Ann Thorac Surg* 2005;79:e1–e2.
22. van Bodegom PC, Wagenaar SS, Corrin B, et al. Second primary lung cancer: importance of long term follow up. *Thorax* 1989;44:788–793.
23. Verhagen AF, Tavilla G, van de Wal HJ, et al. Multiple primary lung cancers. *Thorac Cardiovasc Surg* 1994;42:40–44.
24. Rosengart TK, Martini N, Ghosn P, et al. Multiple primary lung carcinomas: prognosis and treatment. *Ann Thorac Surg* 1991;52:773–779.
25. Okada M, Tsubota N, Yoshimura M, et al. Operative approach for multiple primary lung carcinomas. *J Thorac Cardiovasc Surg* 1998;115:836–840.
26. Antakli T, Schaefer RF, Rutherford JE, et al. Second primary lung cancer. *Ann Thorac Surg* 59:863–866, 1995; discussion 867.
27. Matsuzoe D, Hideshima T, Ohshima K, et al. Discrimination of double primary lung cancer from intrapulmonary metastasis by p53 gene mutation. *Br J Cancer* 1999;79:1549–1552.
28. Osaki T, Oyama T, Takenoyama M, et al. Assessment of prognosis and p53 mutations in patients with multiple tumors of the lung; intrapulmonary metastasis or double primary cancers? *Kyobu Geka* 2002;55:25–29 (Article in Japanese).

Disease-Free Interval Length Correlates to Prognosis of Patients Who Underwent Metastasectomy for Esophageal Lung Metastases

Satoshi Shiono, MD, Masafumi Kawamura, MD,† Toru Sato, MD,* Ken Nakagawa, MD,‡ Jun Nakajima, MD,§ Ichiro Yoshino, MD,‖ Norihiko Ikeda, MD,¶ Hirotoshi Horio, MD,# Hirohiko Akiyama, MD,** and Koichi Kobayashi, MD†; The Metastatic Lung Tumor Study Group of Japan*

Background: Pulmonary metastasectomy is a standard method for treatment of selected pulmonary metastases cases. Nevertheless, because prognosis for patients with lung metastases from esophageal cancer who have undergone pulmonary metastasectomy is poor, candidates for this method of treatment are rare. Therefore, the efficacy of surgical treatment for pulmonary metastatic lesions from esophageal cancer has not been thoroughly examined.

Methods: Between March 1984 and May 2006, 57 patients underwent resection of pulmonary metastases from primary esophageal cancer. These cases were registered in the database developed by the Metastatic Lung Tumor Study Group of Japan and were retrospectively reviewed from the registry. After excluding eight cases because of missing information, we reviewed the remaining 49 cases and examined the prognostic factors for pulmonary metastasectomy for metastases from esophageal cancer.

Results: There were no perioperative deaths. After pulmonary metastasectomy, disease recurred in 16 (33%) of the 49 patients. The overall 5-year survival was 29.6%. Median survival time was 18 months. The survival of patients with a disease-free interval (DFI) less than 12 months was significantly lower than patients with a DFI greater than 12 months. Through multivariate analysis, we identified DFI as a clinical factor significantly related to overall survival ($p = 0.04$).

Conclusions: We identified that patients with a DFI less than 12 months who underwent pulmonary metastasectomy for metastases from esophageal cancer had a worse prognosis. Pulmonary metastasectomy for esophageal cancer should be considered for selected patients with a DFI ≥12 months.

Key Words: Esophageal cancer, Pulmonary metastasis, Metastasectomy.

(*J Thorac Oncol.* 2008;3: 1046–1049)

Pulmonary metastasectomy is a standard method of treatment for selected pulmonary metastases cases.[1] When patients are appropriately selected for this treatment, the overall 5-year survival after pulmonary metastasectomy is about 30 to 40%.[1,2] In general, because prognosis for patients who have undergone this method of treatment is poor with disease frequently recurring, pulmonary metastasectomy is not a frequently chosen method of treatment for lung metastases from esophageal cancer. Consequently, survival after surgery for pulmonary metastases from esophageal cancer has not been thoroughly examined. In Japan, the annual report by the Japanese Association for Thoracic Surgery does not document patients who underwent metastasectomy for metastasized esophageal cancer.[3] Because the outcome of pulmonary metastasectomy for metastases from esophageal cancer has not been thoroughly investigated, it is controversial whether surgery is an effective treatment for metastatic esophageal cancer. To identify prognostic factors of pulmonary metastasectomy for metastases from esophageal cancer, in the present study, we reviewed cases registered in the Metastatic Lung Tumor Study Group of Japan database of patients who underwent metastasectomy for metastasized esophageal cancer.

PATIENTS AND METHODS

The Metastatic Lung Tumor Study Group of Japan developed a database for registration of lung metastases cases. These patients all underwent surgical resection. The database documents the following parameters: gender; age; histology; status of the primary tumor; treatment for the primary tumor; date of primary surgery; kind of surgery; curability; date of metastasis; disease-free interval (DFI); side, size and numbers of resected metastases; date of metas-

*Department of Thoracic Surgery, Yamagata Prefectural Central Hospital, Yamagata, Japan; †Department of Thoracic Surgery, Keio University School of Medicine; ‡Department of Chest Surgery, Cancer Institute Hospital; §Department of Cardiothoracic Surgery, University of Tokyo, Tokyo, Japan; ‖Department of Thoracic Surgery, Chiba University, Chiba, Japan; ¶Department of First Surgery, Tokyo Medical University; #Department of General Thoracic Surgery, Tokyo Metropolitan Komagome Hospital, Tokyo, Japan; and **Department of Thoracic Surgery, Saitama Cancer Center, Saitama, Japan.

Disclosure: The authors declare no conflict of interest.

Address for correspondence: Satoshi Shiono, MD, Department of Thoracic Surgery, Yamagata Prefectural Central Hospital, 1800, Oazaaoyagi, Yamagata 990-2292, Japan. E-mail: sshiono@ypch.gr.jp

ISSN: 1556-0864/08/0309-1046

tasectomy; and follow-up. Between March 1984 and May 2006, 57 patients underwent resection of pulmonary metastases from primary esophageal cancer. These cases were registered in the Metastatic Lung Tumor Study Group of Japan database and were retrospectively reviewed from the registry. Preoperative examination, surgical indication, and operative procedure were at the discretion of each institution.

After excluding eight cases because of missing information such as number of resected metastases, age, or DFI, we examined the remaining 49 cases (46 males and 3 females) in our study. Surgery alone for the primary tumor was performed in 26 cases (53%), surgery and chemoradiotherapy were performed in 7 cases (14%), surgery and radiotherapy were performed in 6 cases (12%), surgery and chemotherapy were performed in 3 cases (6%), radiotherapy alone was performed in 2 cases (4%), and treatment data were not available for 5 cases (10%). We examined the following variables (Table 1): age (≥70 or <70), number of resected metastases (solitary or multiple), resected side (unilateral or bilateral), tumor size (≥3 or <3cm), DFI (≥12 or <12 months), surgical procedure (partial resection, segmentectomy, or lobectomy), and curability (complete or incomplete).

The present study was analyzed using anonymized data that were collected in each institution. Therefore, informed consent was not specifically obtained and institutional review board approval was not necessary.

Statistical Analysis

Overall survival was analyzed by the Kaplan-Meier method, and differences in variables were calculated by the log-rank test. The date of pulmonary resection was defined as the starting point. Cox's proportional hazards model was used for multivariate analysis. The data were calculated using version 5.0 of the StatView software package (SAS Institute Inc, Cary, NC). A p value of less than 0.05 was defined as indicative of statistical significance.

TABLE 1. Survival of 49 Patients According to Clinical Factors of Pulmonary Metastases

Variables	n (%)	5-yr Survival (%)	p
Age (yr)			
≥70	13 (27)	32.9	0.928
<70	36 (73)	27.8	
Number			
Solitary	39 (80)	27.4	0.797
Multiple	10 (20)	42.9	
Resected side			
Unilateral	44 (90)	29.3	0.621
Bilateral	5 (10)	30.0	
Tumor size[a]			
≥3 cm	10 (21)	40.0	0.640
<3 cm	38 (79)	26.7	
DFI			
≥12 mo	28 (57)	39.2	0.048
<12 mo	21 (43)	15.7	
Surgical procedure			
Partial and segment	31 (63)	36.4	0.338
Lobectomy	18 (37)	22.9	
Curability			
Complete	45 (92)	31.4	0.990
Incomplete	4 (8)	25.0	

[a] No cases were available.
DFI, disease-free interval.

RESULTS

The median interval between treatment of esophageal cancer and diagnosis of pulmonary metastasis (disease-free interval) was 14 months (range: 0–124 months). There were no perioperative deaths. The median age of patients at the time of pulmonary metastasectomy was 65 years (range: 35–82). The median number of resected metastatic lesions per patient was one (range: 1–5). The metastases ranged in size from 0.4 to 5.5 cm, and the median size was 2.0 cm. The metastases were squamous cell carcinoma in 48 cases and adenocarcinoma in one case. The surgical procedure was wedge resection in 23 cases (47%), lobectomy in 16 cases (33%), segmentectomy in 8 cases (16%), and bilobectomy in 2 cases (4%). The median follow-up period after the first pulmonary resection was 18 months (range: 0–206 months). Recurrence developed in 16 (33%) of the 49 patients. Recurrences were as follows: lung, nine; lymph node, three; neck, one; distant metastasis, one; stomach, one; and unknown, two. The overall 5-year survival after pulmonary metastasectomy was 29.6% (Figure 1). Median survival time was 27 months. We investigated the relationships between prognostic factors and survival (Table 1). Patients with a DFI less than 12 months had a significantly worse prognosis, as assessed by survival rates, than patients with a DFI greater than 12 months (Figure 2). Multivariate analysis of these variables was performed using Cox's proportional hazards model for disease-specific survival. A DFI less than 12 months was shown to be an independent prognostic factor ($p = 0.04$) (Table 2). At the time of submission, 28 patients examined in our study have died. Although 23 patients died of esophageal cancer, 7 patients were not available for recurrent sites. Five patients have died of other diseases (two cases

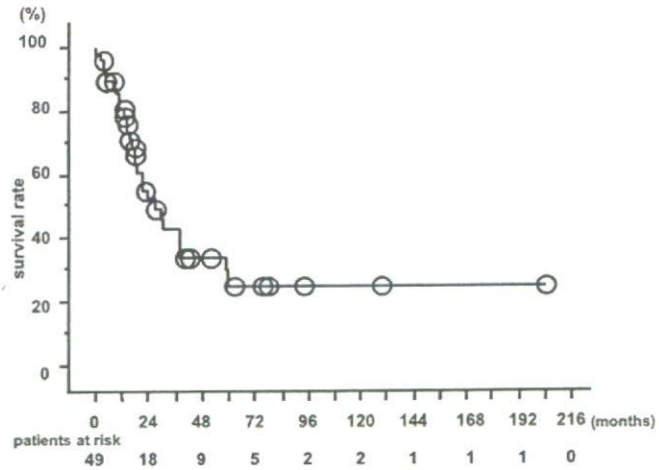

FIGURE 1. Overall survival of the 49 patients after pulmonary metastasectomy. The 5-year survival was 29.6%.

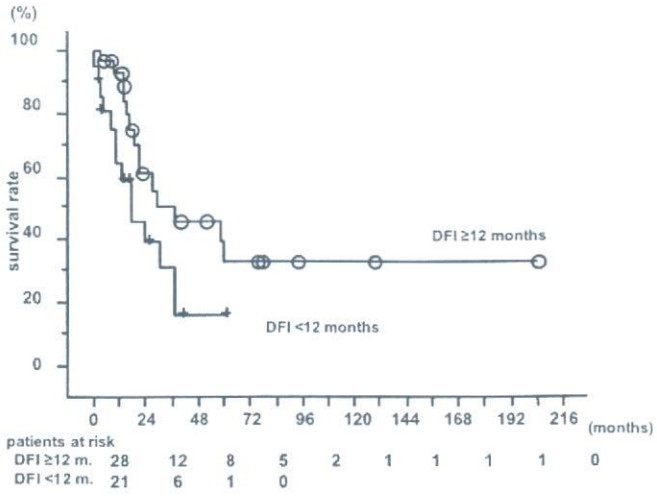

FIGURE 2. Overall survival after pulmonary metastasectomy according to DFI. Survival curves of patients with DFI <12 months and ≥12 months. DFI, disease-free interval.

TABLE 2. Relationships of Individual Variables to Survival (Cox's Proportional Hazards Model)

Variable	Risk Ratio	95% CI	*p*
≥70 yr	1.01	0.41–2.50	0.983
Multiple metastasis	1.67	0.30–9.19	0.557
Bilateral metastasis	1.19	0.19–7.53	0.853
Tumor size ≥3 cm	0.76	0.25–2.35	0.635
DFI <12 mo	2.30	1.04–5.09	0.040
Partial and segment	0.60	0.22–1.65	0.180
Incomplete resection	1.00	0.22–4.56	0.881

CI, confidence interval; DFI, disease-free interval.

were pneumonia, two cases were cerebral infarction, and one case was myocardial infarction).

DISCUSSION

Patients who are candidates for pulmonary metastasectomy for metastases from esophageal cancer are a minority. Analysis of the outcomes of surgery for pulmonary metastases from esophageal cancer has not been published. Quint et al.[4] showed that 29 of 147 (20%) patients with newly diagnosed metastasized esophageal cancer had lung metastasis. Although autopsy studies showed that the frequency of esophageal lung metastasis was 50%,[5] there was not a high percentage of esophageal cancer relapse after esophagectomy. Kyriazanos et al.[6] revealed that 12 of 151 (8%) patients who underwent a curative esophageal resection had lung metastases. Within our study the number of adenocarcinoma of the esophagus was very small. Because the frequency of adenocarcinoma of the esophagus is low in Japan, we do not speculate about the scarce incidence of lung metastasis from adenocarcinoma of the esophagus.

Matsubara et al. showed that 38 of 230 patients (17%) who underwent surgery for esophageal cancer with extended lymph node dissection had distant metastases and 14 (6%) patients had lung metastases. In their article, the outcomes after recurrence were dismal, and no patients were alive 5 years after detection of recurrence. Nevertheless, they showed that the 1-year survival of the patients who had recurrent lesions and were treated with resection and adjuvant therapy was 83%. They concluded that when recurrent lesions were localized macroscopically, surgical removal of the recurrent lesions was an effective treatment.[7] Through our analysis, we found a 5-year survival of 29.6% after pulmonary metastasectomy, which indicates that pulmonary metastasectomy is a promising treatment for metastases from esophageal cancer. Nevertheless, as it is not easy to differentiate esophageal metastases from primary lung squamous cell carcinomas, it is possible that our data might include primary lung squamous cell carcinoma. Survival after metastasectomy might be lower than what our data indicate. Virgo et al mentioned that genetic markers are needed to confidently distinguish between metastases and primary solitary nodules.[8] Further investigation is needed to clarify this matter.

An article from the international registry of lung metastases states that the 5-year survival was 37% after pulmonary metastasectomy. In addition, the article showed that among cases of complete resection, the 5-year survival was 33% for patients with a DFI of 0 to 11 months and 45% for those with a DFI of more than 36 months. Furthermore, the 5-year survival was 43% for single lesions and 27% for 4 or more lesions.[1] DFI and number of pulmonary metastases are significant prognostic factors. Because our present data show that the median DFI is 14 months, we categorized DFI as ≥12 or <12 months. Regarding the DFI, our study suggests that patients with a DFI less than 12 months have a poor prognosis. Osugi et al. showed that 83% of recurrences presented within 24 months after esophagectomy and that the chance of survival of patients whose disease recurred within 24 months after esophagectomy was better than that of patients who suffered recurrence within 24 months. Regarding follow-up studies after esophagectomy, meticulous care should be taken to detect hematogenous recurrence.[9]

In general, incomplete resection is a dismal prognostic factor in lung metastasectomy. We could not demonstrate whether surgical curability is a prognostic factor. McDonald et al. reported that incomplete resection appeared to have no influence on overall survival in metastatic breast cancer. They suggested that this could be due to the systemic nature of the disease at the time of thoracotomy with unsuspected occult metastasis in other areas.[10] Nevertheless, in our study, only four patients underwent incomplete resection. Because the report from The International Registry of Lung Metastases stated that cases with incomplete resection clearly had worse prognoses,[1] we speculate that patients with lung metastases from esophageal cancer have the same tendency.

Although our present study was multi-institutional, we could not analyze in detail all of the records for each patient. From this point of view, because our findings were based on a limited number of cases, pulmonary metastasectomy for lung metastases from esophageal cancer is still highly controversial. Nevertheless, we identified that patients with a DFI less than 12 months had a worse prognosis, as assessed by

survival rates, than patients with a DFI greater than 12 months.

Consequently, although metastases from esophageal cancer are a minority, we think that pulmonary metastasectomy for esophageal cancer should be considered for selected patients with a DFI ≥12 months. As this study is small, further clinical studies will be needed.

REFERENCES

1. Pastorino U, Buyse M, Friedel G, et al. Long-term results of lung metastasectomy: prognostic analyses bases on 5206 cases. *J Thorac Cardiovasc Surg* 1997;113:37–49.
2. Kondo H, Okumura T, Ohde Y, Nakagawa K. Surgical treatment for metastatic malignancies. Pulmonary metastasis: indications and outcomes. *Int J Clin Oncol* 2005;10:81–85.
3. Kazui T, Osada H, Fujita H. Thoracic and cardiovascular surgery in Japan during 2004. *Jpn J Thorac Cardiovasc Surg* 2006;54:363–385.
4. Quint LE, Hepburn LM, Francis IR, Whyte RI, Orringer MB. Incidence and distribution of distant metastases from newly diagnosed esophageal carcinoma. *Cancer* 1995;76:1120–1125.
5. Anderson LL, Lad TE. Autopsy findings in squamous-cell carcinoma of the esophagus. *Cancer* 1982;50:1587–1590.
6. Kyriazanos ID, Tachibana M, Shibakita M, et al. Pattern of recurrence after extended esophagectomy for squamous cell carcinoma of the esophagus. *Hepatogastroenterology* 2003;50:115–120.
7. Matsubara T, Ueda M, Takahashi T, Nakajima T, Nishi M. Localization of recurrent disease after extended lymph node dissection for carcinoma of the esophagus. *J Am Coll Surg* 1996;182:340–346.
8. Virgo KS, Naunheim KS, Johnson FE. Preoperative workup and postoperative surveillance for patients undergoing pulmonary metastasectomy. *Thorac Surg Clin* 2006;16:125–131.
9. Osugi H, Takemura M, Higashino M, et al. Causes of death and pattern of recurrence after esophagectomy and extended lymphadenectomy for squamous cell carcinoma of the thoracic esophagus. *Oncol Rep* 2003; 10:81–87.
10. McDonald ML, Deschamps C, Ilstrup DM, Allen MS, Trastek VF, Pairolero PC. Pulmonary resection for metastatic breast cancer. *Ann Thorac Surg* 1994;58:1599–1602.

VOLUME 26 · NUMBER 4 · FEBRUARY 1 2008

JOURNAL OF CLINICAL ONCOLOGY

ORIGINAL REPORT

Phase II Trial of Preoperative Chemoradiotherapy Followed by Surgical Resection in Patients With Superior Sulcus Non–Small-Cell Lung Cancers: Report of Japan Clinical Oncology Group Trial 9806

Hideo Kunitoh, Harubumi Kato, Masahiro Tsuboi, Taro Shibata, Hisao Asamura, Yukito Ichinose, Nobuyuki Katakami, Kanji Nagai, Tetsuya Mitsudomi, Akihide Matsumura, Ken Nakagawa, Hirohito Tada, and Nagahiro Saijo

From the Department of Medical Oncology and Division of Thoracic Surgery, National Cancer Center Hospital, Department of Thoracic Surgery, Tokyo Medical University; Japan Clinical Oncology Group Data Center, Center for Cancer Control and Information Services, National Cancer Center; Department of Thoracic Surgery, Cancer Institute Hospital, Tokyo; Department of Chest Surgery, National Kyushu Cancer Center, Fukuoka; Pulmonary Unit, Kobe City Medical Center General Hospital, Kobe; Department of Thoracic Surgery, National Cancer Center Hospital East, Kashiwa; Department of Thoracic Surgery, Aichi Cancer Center Hospital, Nagoya; Department of Surgery, National Hospital Organization Kinki-Chuo Chest Medical Center, Sakai; and Department of Thoracic Surgery, Osaka City General Hospital, Osaka, Japan.

Submitted September 1, 2007; accepted October 25, 2007.

Supported by the Grant-in-Aid for Cancer Research from the Ministry of Health, Labour and Welfare of Japan (Grants No. 11S-2, 11S-4, 14S-2, 14S-4, 17S-2, and 17S-5).

Presented in part at the 39th Annual Meeting of the American Society of Clinical Oncology, May 31-June 3, 2003, Chicago, IL, and at the 11th World Conference on Lung Cancer, July 3-6, 2005, Barcelona, Spain.

Authors' disclosures of potential conflicts of interest and author contributions are found at the end of this article.

Corresponding author: Hideo Kunitoh, MD, Department of Medical Oncology, National Cancer Center Hospital, 5-1-1 Tsukiji, Chuo-ku, Tokyo 104-0045, Japan; e-mail: hkkunito@ncc.go.jp.

0732-183X/08/2604-644/$20.00

DOI: 10.1200/JCO.2007.14.1911

ABSTRACT

Purpose
To evaluate the safety and efficacy of preoperative chemoradiotherapy followed by surgical resection for superior sulcus tumors (SSTs).

Patients and Methods
Patients with pathologically documented non–small-cell lung cancer with invasion of the first rib or more superior chest wall were enrolled as eligible; those with distant metastasis, pleural dissemination, and/or mediastinal node involvement were excluded. Patients received two cycles of chemotherapy every 4 weeks as follows; mitomycin 8 mg/m^2 on day 1, vindesine 3 mg/m^2 on days 1 and 8, and cisplatin 80 mg/m^2 on day 1. Radiotherapy directed at the tumor and the ipsilateral supraclavicular nodes was started on day 2 of each course, at the total dose of 45 Gy in 25 fractions, with a 1-week split. Thoracotomy was undertaken 2 to 4 weeks after completion of the chemoradiotherapy. Those with unresectable disease received boost radiotherapy.

Results
From May 1999 to November 2002, 76 patients were enrolled, of whom 20 had T4 disease; 75 patients were fully assessable. Chemoradiotherapy was generally well tolerated. Fifty-seven patients (76%) underwent surgical resection, and pathologic complete resection was achieved in 51 patients (68%). There were 12 patients with pathologic complete response. Major postoperative morbidity, including chylothorax, empyema, pneumonitis, adult respiratory distress syndrome, and bleeding, was observed in eight patients. There were three treatment-related deaths, including two deaths owing to postsurgical complications and one death owing to sepsis during chemoradiotherapy. The disease-free and overall survival rates at 3 years were 49% and 61%, respectively; at 5 years, they were 45% and 56%, respectively.

Conclusion
This trimodality approach is safe and effective for the treatment of patients with SSTs.

J Clin Oncol 26:644-649. © 2008 by American Society of Clinical Oncology

INTRODUCTION

Superior sulcus tumors (SSTs), involving structures at the thoracic inlet, represent a small subtype of non–small-cell lung carcinoma (NSCLC). These SSTs, first described by Henry Pancoast[1,2] and thus also called Pancoast tumors, have posed a challenging problem for surgeons, radiation oncologists, and medical oncologists alike, ever since they were first described.[3]

Preoperative radiotherapy has long been the community standard in the management of SSTs.[4-17] However, both the complete resection rate (approximately 50%) and long-term survival rate (approximately 30%) have remained poor and unchanged over the last 40 years, since the first treatment strategy was reported in the 1960s. Local control has remained the main problem,[15,17,18] adversely affecting quality of life as well as survival of patients. Presence of mediastinal lymph node metastasis (N2 status) has been reported to be associated with a particularly poor prognosis.[9,18]

However, a series of clinical trials over the last two decades have shown concurrent chemoradiotherapy to be beneficial in the treatment of unresectable stage III NSCLC.[19-21] The addition of chemotherapy to thoracic radiotherapy seems to suppress distant micrometastases,[22,23] and giving